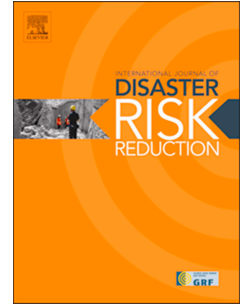


Journal Pre-proof

Operational Status Effect on the Seismic Risk Assessment of Oil Refineries

Vasileios E. Melissianos, Nikolaos D. Karaferis, Konstantinos Bakalis, Athanasia K. Kazantzi, Dimitrios Vamvatsikos



PII: S2212-4209(24)00604-6

DOI: <https://doi.org/10.1016/j.ijdr.2024.104842>

Reference: IJDRR 104842

To appear in: *International Journal of Disaster Risk Reduction*

Received Date: 26 June 2024

Revised Date: 17 September 2024

Accepted Date: 17 September 2024

Please cite this article as: V.E. Melissianos, N.D. Karaferis, K. Bakalis, A.K. Kazantzi, D. Vamvatsikos, Operational Status Effect on the Seismic Risk Assessment of Oil Refineries, *International Journal of Disaster Risk Reduction*, <https://doi.org/10.1016/j.ijdr.2024.104842>.

This is a PDF file of an article that has undergone enhancements after acceptance, such as the addition of a cover page and metadata, and formatting for readability, but it is not yet the definitive version of record. This version will undergo additional copyediting, typesetting and review before it is published in its final form, but we are providing this version to give early visibility of the article. Please note that, during the production process, errors may be discovered which could affect the content, and all legal disclaimers that apply to the journal pertain.

© 2024 Published by Elsevier Ltd.

Operational Status Effect on the Seismic Risk Assessment of Oil Refineries

Vasileios E. Melissianos¹, Nikolaos D. Karaferis¹, Konstantinos Bakalis¹, Athanasia K. Kazantzi², Dimitrios Vamvatsikos¹

¹School of Civil Engineering, National Technical University of Athens, Athens, Greece

²Department of Civil Engineering, School of Engineering, University of Birmingham, Birmingham, UK

Corresponding Author: Vasileios E. Melissianos, School of Civil Engineering, National Technical University of Athens, Heron Polytehneiou 9, Politehneiupoli, 15772 Zografos, Attika, Greece, email: melissia@mail.ntua.gr

Abstract: The operational status of an oil refinery (type and scale of operations that take place at any time instance) largely determines the amount of fuel that is produced, circulated within the facility, and stored in tanks. This status is affected by seasonality, periods of peak or low demand, as well as periods of routine maintenance. However, it is an aspect that is typically neglected even though it stands out among the factors that determine the seismic performance of several critical industrial assets, such as the storage tanks, as well as the consequences of any potential failure. An open-data refinery testbed is employed herein to demonstrate the effect of the refinery's operational status on the seismic risk estimates. Alternative realistic operational scenarios are developed following typical industry practices and are arranged over a time period between two refinery major maintenance shutdown events. The most probable damage state is selected for each asset to identify the most vulnerable ones. Based on the type and importance of the impacted assets, the potential consequences are determined at the facility level. Resulting estimates are very different if an earthquake strikes during a regular/high/low-demand period, or during a maintenance period. The framework can be utilized to identify the locations within the refinery that may trigger cascading failures and secondary damages, should their assets be damaged by a seismic event. The outcomes can be exploited by stakeholders, risk engineers, and emergency action planners for developing customized and businesslike procedures to enhance the seismic resilience of the facility.

Keywords: oil refinery, earthquake, risk assessment, operational status

34 1. Introduction

35 Crude oil refineries are critical energy infrastructures that play a determinant role in the
36 economy, both at a regional and national scale. Large amounts of flammable, toxic, and
37 explosive materials are produced, circulated, and stored within the refineries. In case of
38 earthquake-induced damages, the consequences may be disastrous, spanning from injuries and
39 fatalities to environmental pollution, direct and long-term monetary losses, as well as downtime
40 [1]. Refineries are designed, constructed, operated, and maintained through a grid of strict
41 regulations aiming to ensure their structural and operational integrity even when they are
42 affected by large earthquake events since they are classified as major-risk facilities according
43 to the Seveso-III Directive [2]. Nevertheless, seismically-triggered Natural-Technological
44 (NaTech) accidents still occur. For example, after the 1991 Costa Rica [3], the 1999 Kocaeli,
45 Türkiye [4] and the 2011 Great East Japan [5] earthquakes, several oil storage facilities, and
46 power plants were heavily damaged [6,7], resulting in the contamination of huge farmlands.
47 The disastrous results of seismically-triggered failures of refineries and industrial facilities in
48 the 2000s (e.g., the 2003 Bam, Iran [8], the 2006 Silakhor, Iran [9], the 2008 Wenchuan, PRC
49 [10], the 2010 Chile [11], the 2012 Emilia Romagna, Italy [12], and 2023 Türkiye [13]
50 earthquakes) and in particular the 2011 accident at the Fukushima Nuclear Power Plant [14,15]
51 forced the international community to take action. This resulted in the Sendai Framework for
52 Disaster Risk Reduction [16] that sets up guidelines for risk reduction in critical infrastructure,
53 such as oil refineries [17]. Refinery designers, operators, and stakeholders are cooperating with
54 regulatory authorities to develop and update a comprehensive framework for risk assessment
55 of industrial facilities in case of NaTech events [18]. This framework includes risk identification
56 and analysis [19], risk evaluation [20], and risk rating [21,22]. However, these analysis tools
57 and procedures are generally qualitative and do not offer the necessary information to compute
58 seismic losses and resilience. Still, they are useful to develop a preliminary mitigation strategy
59 using, for instance, accident analysis and risk analysis tools [19].

60 Taking a step towards the quantification of seismic risk for community-critical
61 infrastructure, research efforts are shifting towards a performance-based methodology [23]. The
62 latter is systematically adopted for individual refinery assets, such as tanks [24–32], high-rise
63 stacks [33–36], buildings supporting equipment [37–42], and pipe racks [43–49] among others.
64 Regarding industrial facilities, research efforts have recently intensified, starting from the
65 integration of seismic hazard into typical Quantitative Risk Analysis (QRA) [22,50]. Girgin and
66 Krausmann [51] developed an online tool for the rapid risk assessment of NaTech events at
67 local and regional scales. Bursi et al. [52] presented a probabilistic seismic analysis of an LNG
68 subplant, employing detailed finite element modeling for the critical assets. Alessandri et al.
69 [53] developed a detailed framework for the probabilistic analysis of process plants based on
70 Monte Carlo simulations. Their analysis includes multiple accident chains, consequences
71 analysis, and risk computation, all of which were tested on a tank farm. Caputo et al. [54]
72 systematically reviewed the seismic QRA of chemical process plants. They concluded that the
73 next required steps in the pertinent scientific field are the consistent handling of uncertainties,
74 the introduction of temporal event sequence, the reliable estimation of loss functions, and the
75 quantification of resilience. On account of the above, Caputo et al. [55] developed a
76 methodology to estimate the seismic resilience of process plants, assessing the capacity and
77 economic losses, as well as the time needed for recovery following earthquake events.
78 Furthermore, Huang et al. [56] employed Monte Carlo simulation within QRA, accounting for

79 alternative stress scenarios in a chemical tank farm, incorporating the equipment's importance
80 level and the event trees of failures to eventually compute the probability of failures caused by
81 domino effects. Corritore et al. [57] focused their research on identifying the most vulnerable
82 (and critical) assets in major-hazard facilities in case of an earthquake to improve existing
83 QRAs. Kalemi et al. [58] developed a framework for the probabilistic seismic resilience
84 analysis of process plants that includes the process mapping, the definition of the initial plant
85 capacity, the formulation of the plant recovery model, and the definition of a resilience index
86 and economic loss model. Wang et al. [59] developed a quantitative assessment framework for
87 the seismic resilience of petroleum depots by explicitly considering the interactions between
88 the components and the subsystems with the overall system/facility. O'Reilly et al. [60]
89 presented their work on a risk-aware navigation system within industrial plants subjected to
90 earthquake-triggered NaTech events by incorporating the input from a grid of sensors
91 (accelerometers, fiber optic sensors, and weather stations). Finally, Karastathis et al. [61]
92 presented an early warning system for protecting oil refineries in case of an earthquake, using
93 a network of accelerometers to detect earthquake events in the surrounding area and provide
94 visual rapid assessment of the expected damages.

95 Owing to the above, it is evident that the research community has made decisive steps
96 toward establishing a framework to compute the seismic resilience of process plants. Still, the
97 following gaps in the existing literature can be identified: (1) lack of a framework that is suitable
98 for examining an entire crude oil refinery as an integrated system, (2) lack of a transparent
99 methodology for considering the impact that the failure of a particular asset could have on the
100 functionality of the entire system, and (3) lack of a framework for assessing the operational
101 status of the refinery.

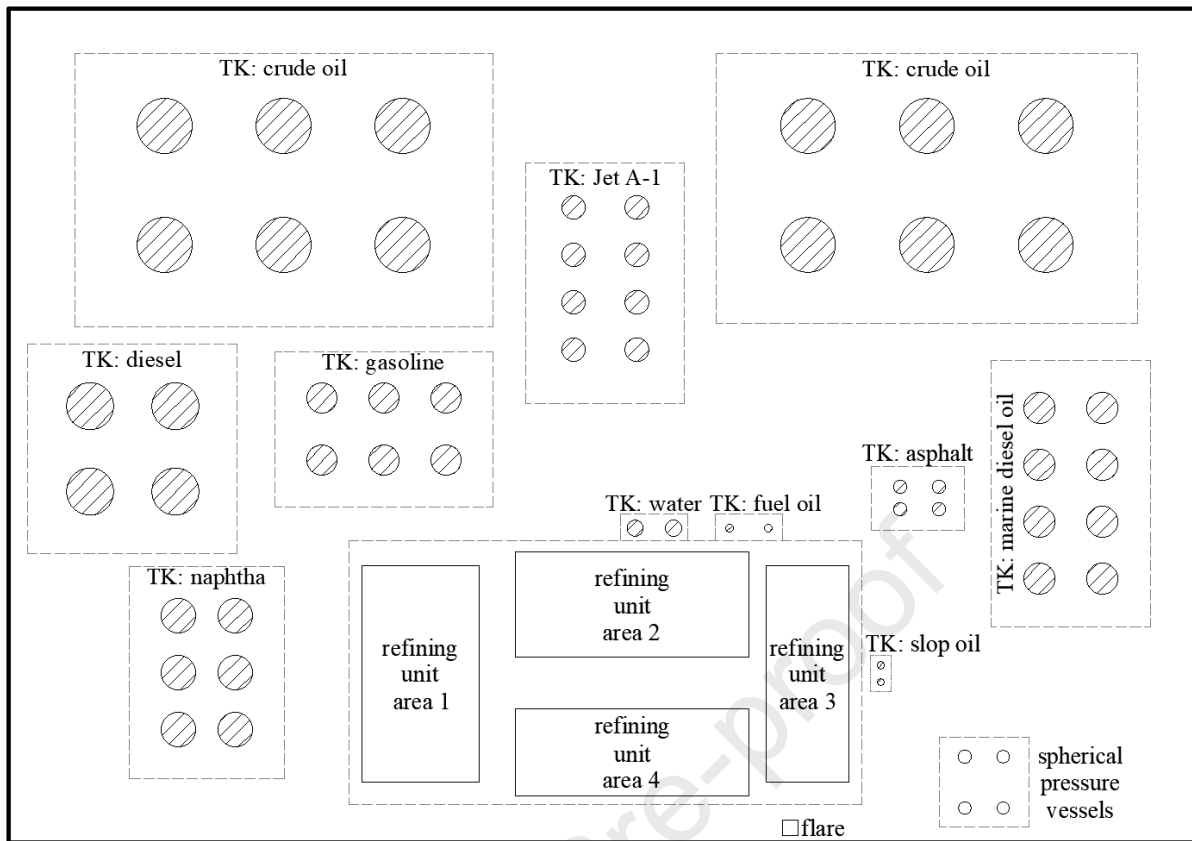
102 To help foster further research in the field, the authors have recently formulated an open-
103 data virtual crude oil refinery testbed, located in a high-seismicity region of Greece, to
104 consequently develop and test system-level assessment methods [62]. The testbed includes the
105 following: (a) all critical assets, the potential failure of which is prioritized according to their
106 impact on plant functionality; (b) the overall layout of the refinery since the location of the
107 individual assets is critical when examining cascading failures (currently out-of-scope of this
108 study), i.e., the initiation of a fire and its propagation to other assets that may or may have not
109 been damaged by the earthquake; and (c) the parameters that govern the response of tanks (e.g.,
110 size, fill ratio, and content density), as they largely determine the direct consequences and their
111 cascading effects; for example, the approach to extinguishing a fire in a crude oil tank differs
112 dramatically from that of a fire in a naphtha tank.

113 In partially addressing the aforementioned issues, the present study focuses on the
114 operational status of the refinery to demonstrate its effect on seismic performance estimates. A
115 series of realistic operation scenarios are developed per typical industrial practices and are
116 analyzed to demonstrate the status of each asset. Moreover, preliminary seismic performance
117 estimates are presented to demonstrate the effect of operational status and identify the most
118 vulnerable asset in each case. The overall goal is to enhance the seismic resilience of refineries
119 by setting the pathway for planning customized and business-like procedures for emergency
120 response actions, as well as preventive measures that account for the actual operation status of
121 the refinery. At the same time, the presented framework sheds light into the refinery sectors
122 where it is more likely to be the onset of cascading failures due to a fire or an explosion as a
123 result of the damages sustained by their most vulnerable assets per scenario.

124 2. Refinery testbed outline

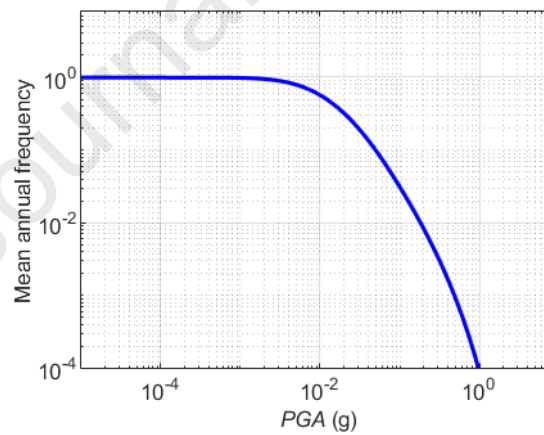
125 As a basis, we employ the open-data testbed developed by the authors [62] to represent
126 a typical mid-sized crude oil refinery. The process plant covers an area of $1850\text{m} \times 1250\text{m}$
127 and its plan view is illustrated in Figure 1. The core of the process plant is the refining unit
128 areas, where all chemical and physical processes take place. In the remaining area, atmospheric
129 liquid-storage tanks, spherical pressure vessels for storing gaseous fuel, such as butane and
130 propane, and the main refinery flare are located. The complete catalog of the assets considered
131 in the exposure model is shown in Table 1. The geometry, the dynamic characteristics, the
132 numerical analysis results, and the fragility curves for all the considered assets are offered in a
133 dedicated repository [63]. The development of the exposure model, which includes the most
134 seismically vulnerable assets, was carried out using a spectrum of approaches, namely,
135 numerical analysis results of assets, literature, and engineering judgment [62]. It should be
136 noted that piping was not considered in the exposure model based on the following
137 considerations: (a) buried steel piping primarily consists of straight segments that can be
138 damaged by transient ground displacements caused by seismic wave propagation under certain
139 conditions related to soil stratigraphy [64]. Uniform soil conditions have been assumed, and
140 therefore, the potential failure of buried pipes due to seismic wave propagation has been
141 excluded. It is important to note that the buried piping network of the refinery is not directly
142 comparable to an urban gas distribution network, which covers a larger (city-level) area with
143 varying geological conditions and is, therefore, more susceptible to seismic-induced permanent
144 and transient ground displacements [65,66]. (b) Above-ground piping is typically supported by
145 sleepers, with or without pendulum-type connectors, while expansion joints, U-type pipe loops,
146 elbows, and bends provide the necessary flexibility for thermal expansion and contraction of
147 the piping. The latter two conditions are more commonly associated with pipe damage. These
148 configurations, along with the inherent flexibility of the piping, enable the system to undergo
149 slight transverse and longitudinal displacements, usually allowing it to safely accommodate the
150 displacements imposed by ground shaking.

151 The refinery is assumed to be located west of Athens, Greece, in a major industrial area.
152 This area is within a high-seismicity region of Greece due to many active faults identified in
153 the Corinth Gulf [67]. Using the 2013 European Seismic Hazard Model [68], the obtained
154 seismic hazard curve for the site of interest is shown in Figure 2, having a 10% in 50yrs value
155 of $0.36g$. Uniform soil conditions have been assumed throughout the facility for the purpose of
156 the test, allowing neglect the ground motion spatial variability, thus applying each ground
157 motion as is to all refinery assets.



158

159 Figure 1: Plan view of the crude oil refinery testbed (adapted from [62]) [TK: liquid storage
 160 tanks].



161

162

Figure 2: Seismic hazard curve at the refinery's site.

163

Table 1: Refinery structures considered in the exposure model of the refinery testbed

Storage assets	No. of assets	Process assets	No. of assets
Gasoline tank	6	Horizontal pressure vessel	8
Fuel oil tank	2	Vertical pressure vessel type CL1	12
Marine diesel oil tank	8	Vertical pressure vessel type CL2	8
Jet A-1 tank	8	Flare	1
Naphtha tank	6	1-story RC building	3
Crude oil tank	12	2-story RC building	17
Diesel tank	4	4-story RC building	7
Slop oil tank	2	1-story steel building	10
Liquid asphalt tank	4	2-story steel building	9
Water tank	2	Process tower	5
Spherical pressure vessel	4	30m steel chimney	3
		80m steel chimney	1
		RC chimney	1

164

165

166

167

168

169

170

171

172

173

174

175

176

177

178

179

180

The susceptibility of individual refinery assets to earthquake damage is identified via asset-specific damage states, which are denoted by lowercase letters “ds”. However, the impact of an asset’s failure – whether operational or structural – varies in significance concerning the overall operational integrity of the refinery. Therefore, it is required to homogenize the asset-level damage states into a set of refinery-level damage states, which are denoted by uppercase letters “DS” in order to accurately reflect their functional consequences. These five distinct global DSs, range from “none” to “severe” disruption and are listed in Table 2. For each DS, the operational status (in terms of functionality) is presented along with the expected extent of repairs that need to be undertaken for the damaged structures in the aftermath of an earthquake. The homogenization process has been carried out considering the following factors: (1) the significance of each asset in the refining process, (2) the potential business disruption consequences (such as downtime and cost) for the entire refinery, (3) the asset's location, (4) potential cascading effects from failure and the spread of damage due to loss of containment and subsequent fires, and (5) expert judgment. It is important to note that, given the significant operational interdependencies among assets and the complexity of the refining process, the failure of a single asset will affect the refinery's functionality, with the extent of the impact depending on a complex interplay of factors that cannot be quantified in this context.

181

182

183

184

185

186

187

188

189

190

191

192

193

It is noted especially that in case DS4 (severe level of disruption) is attained, the refinery may remain partially operational at low capacity while the damage is addressed, or slowly reduce operations in the process of being shut down. As a general remark, one should bear in mind that stopping the refining process takes a lot of time (in the order of a couple of days) and is a procedure with many inherent risks (e.g., fire, explosion, machinery failure, unexpected chemical reaction, etc.) as numerous complex physical and chemical procedures and reaction chains have to be terminated (e.g., [69,70]). In other cases, only an isolated part of a refinery may be damaged and other parts may keep operating at a minimum level. For example, let two or more liquid storage tanks be severely damaged in the aftermath of an earthquake. Assuming that they are located far away from the refining unit areas, the overall production of the facility is significantly reduced until the situation (e.g., material release, fire) is under control. The refinery personnel will need to take all the required measures to ensure the safety of the facility and will thus have to keep some equipment in operation, e.g., moving product away from the

194 damaged areas or even sending it away from the facility via pipelines. Thus, occurrence of DS4
 195 can lead to a multitude of operational outcomes that cannot be addressed without further case-
 196 specific analysis.

197 Table 2: Refinery global Damage States in terms of operational disruption as per [62]

Damage State	DS0	DS1	DS2	DS3	DS4
Level of disruption	None	Low	Moderate	Extensive	Severe
Operational status	—	Refinery is operational at almost 100% capacity	Refinery is operational with some parts at a reduced capacity	Refinery is partially operational at a reduced capacity	Refinery is partially operational at low capacity and may be shut down
Repairs required	—	Some assets require scheduling of minor repairs	Some assets require immediate major repairs	Some assets require extensive repairs	Many assets require extensive repairs and/or replacement

198 3. Refinery operation scenarios

199 The amount of fuel circulated, processed, and stored within the refinery is related to its
 200 operational status. It determines the behavior of the individual structures, essentially dividing
 201 them into two categories (Table 1), namely storage assets and refining process assets. In more
 202 detail:

- 203 • Storage assets include liquid storage tanks and spherical pressure vessels. They are
 204 characterized by their fill ratio (ranging from 0, in the case of empty assets, to 1, in the case
 205 of fully-filled assets), which dominates their structural/dynamic behavior [30,71]. It also
 206 determines the amount of flammable material available at the site. This is a crucial parameter
 207 for estimating any potential post-earthquake cascading consequences. Therefore, it is
 208 deemed necessary to account for the fill ratio of these assets in each considered alternative
 209 scenario for the operational status of the refinery.
- 210 • Process assets that are not related to the storage of final or intermediate fuel products (see
 211 Table 1) are characterized by a binary variable, describing whether they are in operation or
 212 not, depending on the scenario description.

213 To account for the effects of seasonality and periods of maintenance, six alternative
 214 operational scenarios are defined to characterize any day between (and including) major
 215 maintenance actions, so-called turnarounds of the refinery. They are summarized in Table 3 and
 216 are further detailed in the forthcoming sections.

217 Table 3: Refinery operational scenarios.

Scenario No	Description	Remarks
1	Typical day of the year	including minor maintenance
2	Refinery turnaround	major maintenance period
3.1	High-winter time	effect of seasonality
3.2	High-summer time	
4	Low-demand scenario	extreme scenario
5	Peak-demand scenario	extreme scenario

219 3.1. Scenario 1: Typical day of the year

220 The refinery operates under normal capacity within a typical day of the year. The fill
 221 ratio (FR) of the fuel storage assets in this scenario is presented in Table 4. Fuel storage assets
 222 undergo periodic maintenance every 10-15 years unless a non-seismic-related failure (e.g.,
 223 leakage due to extensive corrosion of the steel shell, failure of connected equipment, etc.) is
 224 detected before the scheduled maintenance (see API STD 653:2014 [72]). The duration of this
 225 maintenance period is typically between 6 to 18 months, depending on the properties of the
 226 tanks (i.e., dimensions, material stored), the extent of any non-seismic damage detected, as well
 227 as any potential upgrade of the attached electrical, electronic, and mechanical equipment.
 228 Therefore, especially for a sizeable group of tanks where the same material is stored, it is
 229 reasonable to consider that within a typical day of the year, at least one tank undergoes
 230 maintenance. Furthermore, the following aspects are considered for setting the fill ratios of fuel
 231 storage assets:

- 232 • Regardless of the material stored, at least one or more tanks/vessels will be full for
 233 operational reasons. For example, stored material may be part of a selling contract to a
 234 designated customer.
- 235 • The level of water stored in TK-15 (see Table 4) tanks fluctuate continuously as water is
 236 used in the refining process.
- 237 • The level of slop oil stored in TK-13 (see Table 4) tanks fluctuate continuously, as slop oil
 238 is essentially a waste product of the refining process, which is stored temporarily in tanks
 239 before being sent to the biological cleaning unit for processing that removes environmentally
 240 harmful agents.
- 241 • The amount of material stored in the remaining tanks/vessels can be considered random since
 242 the refining process and selling of products via trucks, pipelines, and the marine terminal (if
 243 any) are continuously progressing.

244 Then, process assets are operational within a typical day of the year.

245 Table 4: Scenario 1 (typical day of the year): Fill ratios of storage assets.

ID	Product	Fill ratio (FR)	No. assets
TK-2	Gasoline	2 with 95%, 3 with random FR, 1 under maintenance	6
TK-3	Fuel oil	2 with random FR	2
TK-5	Marine diesel oil	2 with 95%, 5 with random FR, 1 under maintenance	8
TK-6	Jet A-1	1 with 95%, 6 with random FR, 1 under maintenance	8
TK-8	Naphtha	1 with 95%, 4 with random FR, 1 under maintenance	6
TK-9	Crude oil	3 with 95%, 8 with random FR, 1 under maintenance	12
TK-10	Diesel	1 with 95%, 3 with random FR	4
TK-13	Slop oil	2 with random FR	2
TK-14	Liquid asphalt	1 with 95%, 1 with random FR	2
TK-15	Water	2 with random FR	2
TK-16	Liquid asphalt	1 tank with random FR, 1 under maintenance	2
SPV	Butane & Propane	2 with 95%, 2 with random FR	4

TK: liquid storage tank (numbering refers to specific geometry and content type per [62,63])

SPV: spherical pressure vessel

247 As a remark, in the interval between two turnarounds, partial shutdown for periodic
 248 minor maintenance of one or two refinery processing units typically takes place with its duration
 249 ranging from 30 to 60 days. In such a case, the refinery functionality is slightly reduced but the
 250 rest of the units remain operational. Given the fact that data for the shutdown of individual
 251 refining units is not available and reasonable assumptions cannot be made, it is assumed that
 252 this partial shutdown can be folded into the randomness already assumed in Scenario 1, which
 253 represents a typical day of the year.

254 3.2. Scenario 2: Refinery turnaround

255 The refinery is shut down for major periodic maintenance, a procedure also called
 256 turnaround [73], which typically lasts about two months and takes place every three or four
 257 years [74,75]. Before a turnaround, process units are shut down sequentially for safety and
 258 operational reasons, and afterwards, they are also sequentially restarted. The capacity of the
 259 refinery during the turnaround period is minimal and a limited amount of fuel is circulated. In
 260 that sense, most of the fuel storage assets are full, as presented in Table 5, while a limited
 261 number of them with random FR indicate that the selling of products is still ongoing during the
 262 turnaround period, even at a reduced rate. It should be noted that the level of water stored in
 263 TK-15 and slop oil in TK-13 are considered random given that these tanks are part of the
 264 refining process. During the turnaround period, most of the processing assets will be out of
 265 order. Still, in case of an earthquake, these assets may be damaged. Essentially, in such a case,
 266 the “functionality disruption” presented in Table 2 will be considered as delays in restoring full
 267 operation of the refinery. For example, a catastrophic failure of the flare may not result in an
 268 explosion, fire, etc., because this asset would be out of order during said period. Still, significant
 269 delays would be expected in restarting the facility, signaling a severe functionality disruption.

270 Table 5: Scenario 2 (refinery turnaround): Fill ratio of storage assets.

ID	Product	Fill ratio (FR)	No. assets
TK-2	Gasoline	3 with 95%, 2 with random FR, 1 under maintenance	6
TK-3	Fuel oil	2 with random FR	2
TK-5	Marine diesel oil	5 with 95%, 1 with random FR, 1 with 35%, 1 under maintenance	8
TK-6	Jet A-1	3 with 95%, 2 with random FR, 2 with 35%, 1 under maintenance	8
TK-8	Naphtha	1 with 95%, 4 with 35%, 1 under maintenance	6
TK-9	Crude oil	6 with 95%, 3 with 35%, 2 with random FR, 1 under maintenance	12
TK-10	Diesel	2 with 95%, 2 with 35%	4
TK-13	Slop oil	2 with 35%	2
TK-14	Liquid asphalt	1 with 95%, 1 with 35%	2
TK-15	Water	2 with 95%	2
TK-16	Liquid asphalt	1 with 95%, 1 under maintenance	2
SPV	Butane & Propane	3 with 95%, 1 with 35%	4

TK: liquid storage tank (numbering refers to specific geometry and content type per [62,63])

SPV: spherical pressure vessels

272 3.3. Scenario 3: Effect of seasonality

273 Seasonality does affect the operation of the refinery mainly in terms of the fuel amount
 274 that is stored in tanks [76]. Considering that the examined refinery testbed is located in the
 275 northern hemisphere, the demand for Jet A-1, gasoline, diesel, and marine diesel oil is increased
 276 during summertime due to increased tourism and travel. On the contrary, during wintertime, the
 277 demand for diesel and LPG (stored in spherical pressure vessels) is higher due to the increased
 278 demand for heating. In general, the duration of the relative winter/summertime depends on the
 279 country/region. It should be noted that targeting a finer resolution about seasonal variations,
 280 e.g., to account for the effect of shorter holiday breaks, may be an intriguing but also
 281 challenging objective. To do so properly, would require monitoring, data from everyday
 282 operation, and a statistical analysis of the obtained facility-specific operational data for long
 283 periods of time, e.g., over a decade. It would also require removing the effect of external
 284 parameters that can influence oil prices, such as political decisions, conflict, increase or
 285 reduction of crude oil production, etc. (e.g., [77]). Such a type of analysis is currently out of the
 286 scope of the present study. Moreover, for the same reasons, the daily fluctuation of oil
 287 consumption (e.g., [78]), which is related to the amount of fuel exported from the refinery daily,
 288 is not considered. In that sense, a proxy is proposed to indirectly account for site/region-specific
 289 effects by employing expert opinion to adjust the percentage of high-winter/summer time.

290 Owing to the above, Scenario 3 is subdivided into two discrete cases, namely Scenario
 291 3.1 for high-winter time and Scenario 3.2 for high-summer time. The fill ratio of storage assets
 292 for the high-winter and high-summer scenarios are listed in Table 6 and Table 7, respectively,
 293 indicating the high variation of fill ratios due to the high demand. Finally, the process assets are
 294 typically operational.

295 Table 6: Scenario 3.1 (high-winter time): Fill ratios of storage assets.

ID	Product	Fill ratio (FR)	No. assets
TK-2	Gasoline	3 with 95%, 2 with random FR, 1 under maintenance	6
TK-3	Fuel oil	2 with random FR	2
TK-5	Marine diesel oil	3 with 95%, 4 with random FR, 1 under maintenance	8
TK-6	Jet A-1	4 with 95%, 3 with random FR, 1 under maintenance	8
TK-8	Naphtha	3 with 95%, 3 with random FR	6
TK-9	Crude oil	5 with 95%, 6 with random FR, 1 under maintenance	12
TK-10	Diesel	1 with 95%, 3 with random FR	4
TK-13	Slop oil	2 with random FR	2
TK-14	Liquid asphalt	1 with 95%, 1 with random FR	2
TK-15	Water	2 with random FR	2
TK-16	Liquid asphalt	1 with 95%, 1 with random FR	2
SPV	Butane & Propane	1 with 95%, 3 with random FR	4

TK: liquid storage tank (numbering refers to specific geometry and content type per [62,63])

SPV: spherical pressure vessels

297

Table 7: Scenario 3.2 (high-summer time): Fill ratios of storage assets.

ID	Product	Fill ratio (FR)	No. assets
TK-2	Gasoline	1 with 95%, 5 with random FR	6
TK-3	Fuel oil	2 with random FR	2
TK-5	Marine diesel oil	1 with 95%, 7 with random FR	8
TK-6	Jet A-1	1 with 95%, 7 with random FR	8
TK-8	Naphtha	1 with 95%, 5 with random FR	6
TK-9	Crude oil	3 with 95%, 8 with random FR, 1 under maintenance	12
TK-10	Diesel	1 with 95%, 3 with random FR	4
TK-13	Slop oil	2 with random FR	2
TK-14	Liquid asphalt	1 with 95%, 1 with random FR	2
TK-15	Water	2 with random FR	2
TK-16	Liquid asphalt	2 tanks with random FR	2
SPV	Butane & Propane	2 with 95%, 2 with random FR	4

TK: liquid storage tank (numbering refers to specific geometry and content type per [62,63])

SPV: spherical pressure vessels

298

3.4. Scenario 4: Low-demand scenario

299

Apart from the typical scenarios of the refinery operation examined in Sections 3.1–3.3, it is worth considering an extreme scenario, where the production of the refinery is significantly slowed down due to reduced demand. The latter could be attributed to very high oil prices (e.g., energy crisis) or government-enforced restrictions to travel and transportation (e.g., lockdown due to a pandemic [79]). In such a case, most of the storage assets are expected to be full (Table 8) and thus more vulnerable to earthquake-induced damage [62,71]. Finally, the refinery process assets are typically operational, although the entire production of the refinery is reduced to a mere minimum, due to low demand for oil products.

307

Table 8: Scenario 4 (low demand scenario): Fill ratio of storage assets.

ID	Product	Fill ratio (FR)	No. assets
TK-2	Gasoline	5 with 95%, 1 with random FR	6
TK-3	Fuel oil	2 with random FR	2
TK-5	Marine diesel oil	6 with 95%, 1 with random FR, 1 under maintenance	8
TK-6	Jet A-1	6 with 95%, 1 with random FR, 1 under maintenance	8
TK-8	Naphtha	4 with 95%, 1 with random FR, 1 under maintenance	6
TK-9	Crude oil	9 with 95%, 2 with random FR, 1 under maintenance	12
TK-10	Diesel	3 with 95%, 1 with random FR	4
TK-13	Slop oil	1 with 95%, 1 with random FR	2
TK-14	Liquid asphalt	1 with 95%, 1 with random FR	2
TK-15	Water	2 with random FR	2
TK-16	Liquid asphalt	2 with 95%	2
SPV	Butane & Propane	2 with 95%, 2 with random FR	4

TK: liquid storage tank (numbering refers to specific geometry and content type per [62,63])

SPV: spherical pressure vessels

308

309 3.5. Scenario 5: Peak-demand scenario

310 A peak-demand scenario is also examined. In such a case, the refinery production
 311 capacity is increased to maximum (above normal capacity) to meet the increased market
 312 demand (e.g., post-COVID19 era [80,81]). To that effect, the fill ratio of the tanks can be
 313 considered to be mostly random (see Table 9), as fuel batches move rapidly through the refinery,
 314 filling up and emptying tanks in a (seemingly) random fashion. Finally, the refinery process
 315 assets are typically operational.

316 Table 9: Scenario 5 (peak-demand scenario): Fill ratios of storage assets.

ID	Product	Fill ratio (FR)	No. assets
TK-2	Gasoline	1 with 95%, 4 with random FR, 1 under maintenance	6
TK-3	Fuel oil	2 with random FR	2
TK-5	Marine diesel oil	1 with 95%, 6 with random FR, 1 under maintenance	8
TK-6	Jet A-1	1 with 95%, 6 with random FR, 1 under maintenance	8
TK-8	Naphtha	1 with 95%, 5 with random FR	6
TK-9	Crude oil	2 with 95%, 9 with random FR, 1 under maintenance	12
TK-10	Diesel	1 with 95%, 3 with random FR	4
TK-13	Slop oil	2 with random FR	2
TK-14	Liquid asphalt	2 with random FR	2
TK-15	Water	2 with random FR	2
TK-16	Liquid asphalt	1 with 95%, 1 with random FR	2
SPV	Butane & Propane	2 with 95%, 2 with random FR	4

TK: liquid storage tank (numbering refers to specific geometry and content type per [62,63])

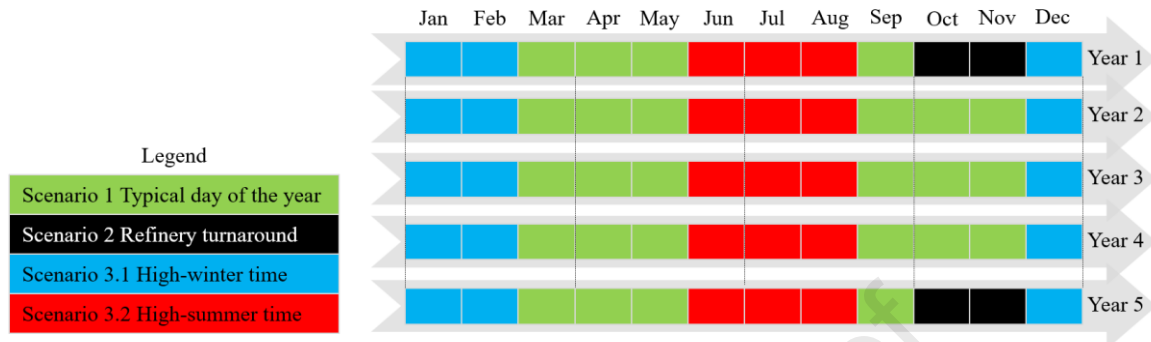
SPV: spherical pressure vessels

317

318 3.6 Refinery operation schedule

319 The examined crude oil refinery testbed is located in Greece, a typical Mediterranean
 320 country, where the weather conditions and local economy influence which of the scenarios
 321 shown in Table 4 – Table 9 is active at any given time. Scenarios 1 to 3 are related to the
 322 “typical” operation of the plant, while extreme Scenarios 4 and 5 cannot be included in the
 323 typical annual operation schedule and are separately examined. Such a schedule is illustrated in
 324 Figure 3 and spans over a 5-year timeframe, where the 4-year time interval between two
 325 successive refinery turnarounds appears. It should be noted that for operational reasons, the
 326 refinery turnaround in the considered oil refinery testbed takes place in October and November,
 327 i.e., between the high-summer and high-winter time periods. Moreover, the high-
 328 summer/winter periods are considered to last roughly 3 months each in the Mediterranean
 329 latitudes, with potential modifications in the future due to the effect of climate change. The
 330 peak- and low-demand scenarios, i.e., Scenarios 4 (Table 8) and 5 (Table 9), respectively, are
 331 treated as random. In other words, it is assumed that there is no *a priori* knowledge of the
 332 occurrence of peak or low demand in the refinery operation. The extreme Scenario 4 of low
 333 demand is assumed to occur at any time over the entire year with a 1% probability; the period
 334 of refinery turnaround is excluded, since turnaround is scheduled and executed typically outside

335 the peak demand periods. Contrarily, the extreme Scenario 5 of peak demand is assumed to
 336 only occur during the high-winter or high-summer time with a 5% probability. Therefore,
 337 Scenario 5 is limited to appearing within the 6 peak months of every year, obviously without
 338 coinciding with refinery turnarounds. It should be noted that the probabilities of occurrence for
 339 extreme Scenarios 5 and 6 are assumptions that have been defined based on expert opinion.



340

341

Figure 3: Typical refinery operation time schedule.

342

343

344

345

346

347

348

349

350

351

352

353

354

355

356

357

358

359

360

361

362

363

364

365

366

367

368

369

The consideration of the operational scenarios allows a fine-grained understanding of the expected status of the refinery assets in the aftermath of an earthquake event. Such detailed information is useful for developing plans and mitigation actions. Still, refinery stakeholders and operators are also interested in seismic risk estimates that are time/scenario-agnostic in the sense that they are not tied to a specific period of the year or corresponding operation scenario. This coarse-grained long-term view of the refinery can be useful for insurance purposes [82]. In that sense, the individual scenarios are aggregated into an “average” year using appropriate annualized weights (AW) that are derived from the typical schedule of the plant (Figure 3) on the 4-year time period that includes a turnaround. It should be noted that AWs are not logic tree weights and are not related to any Bayesian or subjective probability. Actually, AWs represent the annualized probability of scenario occurrence and are listed in Table 10, along with the respective calculation formula. Specifically, 2 months out of 48 are set aside for turnarounds in every four-year period, thus leaving 46 months to be distributed between the remaining five scenarios. In more detail, for the low-demand scenarios, a 1% probability of occurrence over 46 out of 48 months (2 months or turnaround are excluded) yields a computational number of months equal to $0.01 \times (48 - 2) = 0.46$. For the high-demand scenario, a 5% probability of occurrence is considered within the 6 months of winter/summer-time per years, this resulting to a computation number of months equal to $0.05 \times 6 \times 4 = 1.20$. Regarding the typical day, we have 6 months per year from (2 months of turnaround are excluded) which the months of the low-demand scenario (corresponding to the typical day and excluding the high-winter/summer time) have to be deducted, thus resulting to $[(6 \times 4) - 2] - 0.46/2 = 21.77$. The computation months for the refinery turnaround period equal the actual months within the 4-year period, i.e., 2 months. The computational months for the high-winter time equal the ones for the high-summer time. For scenarios 3.1 and 3.2 respectively, we have 3 actual months per year from which those corresponding to low and peak demand are deducted, thus resulting in $(3 \times 4 - 1.20/2 - 0.46 \times 3/12) = 11.285$. Finally, the computational number of months per scenario in the 4-year period is divided by the actual total number of months for this period, namely 48 months, to compute the annualized weight.

370

Table 10: Annualized weights (AWs) of scenarios.

Scenario	Normalized	AW
1 Typical day	21.77/48	0.4535
2 Refinery turnaround	2/48	0.0417
3.1 High-winter time	11.285/48	0.2351
3.2 High-summer time	11.285/48	0.2351
4 Low-demand	0.46/48	0.0096
5 Peak-demand	1.20/48	0.0250
Total		1.0000

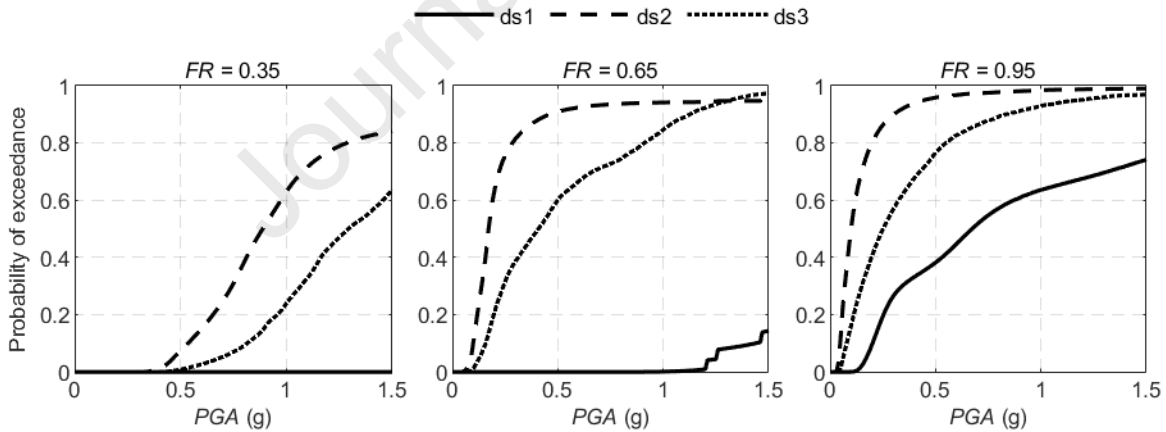
371

372 4. Methodology

373 The refinery status in the aftermath of an earthquake is examined by employing the
 374 seismic fragility curves of the individual assets (see Section 2); the corresponding analytical
 375 fragility curves are offered in the dedicated repository [63] for all assets under examination
 376 [62]. Fragility is defined as [83,84]:

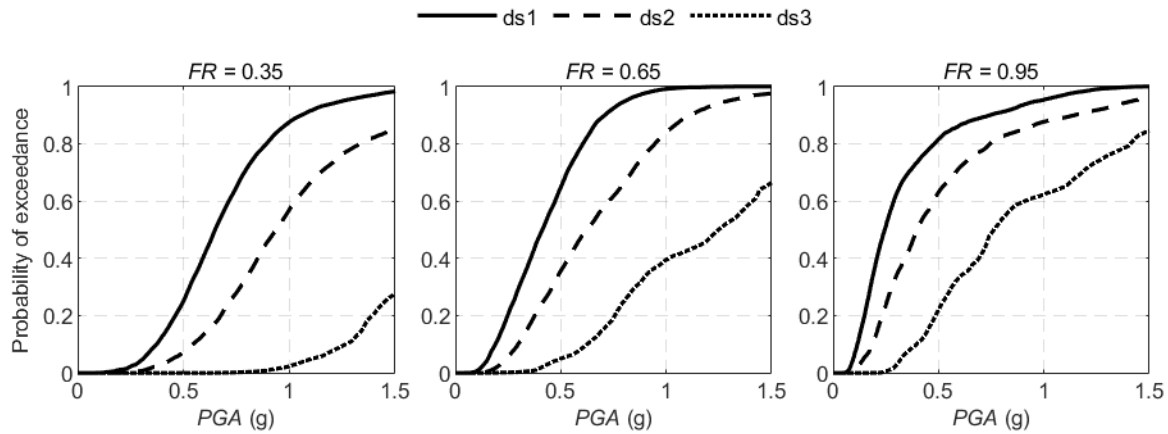
$$F_{LS}(IM) = P[LS \text{ violated}|IM] = P[D > C_{LS}|IM] \quad (1)$$

377 In Equation (1), F_{LS} is the cumulative distribution function, D is the EDP demand and C_{LS} is
 378 the EDP capacity threshold paired to a specific Damage State (DS). Using this definition and
 379 in an attempt to demonstrate the effect of alternative fill ratios on the seismic fragility of storage
 380 assets, the fragility curves of liquid storage tank TK-5 are indicatively presented in Figure 4.
 381 As expected, the higher the fill ratio (FR), the higher the susceptibility to the seismically-
 382 induced damage. Similar conclusions hold for a spherical pressure vessel (Figure 5).



383

384 Figure 4: Liquid storage tank TK-5: Fragility curves for different fill ratios where ds denotes
 385 the asset-specific damage state. The ds2 fragility does not necessarily reach 100% as the
 386 corresponding EDP (base plate plastic rotation) saturates, a feature of the unanchored system
 387 where the “base plate plastic rotation” demand does not present a notable increase with
 388 increasing uplift (or seismic intensity) [30,32]. General note: damage states of liquid storage
 389 tanks are neither sequential nor mutually exclusive; this means that these damage states can be
 390 verified simultaneously in a tank after an earthquake.



391

392 Figure 5: Spherical pressure vessel: Fragility curves for different fill ratios, where ds denotes
 393 the asset-specific damage state.

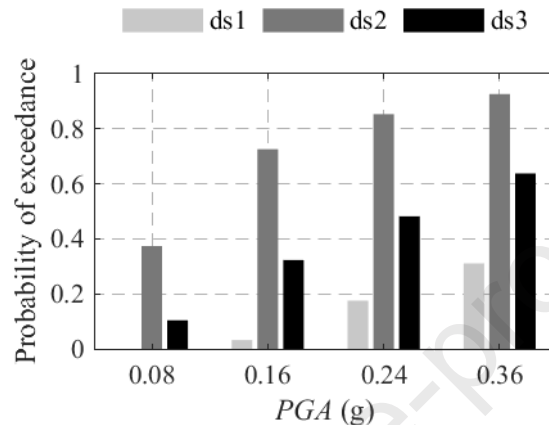
394 The intensity measure (IM) allows the seamless flow of seismic intensity information
 395 for the seismic hazard analysis to the structural analysis. It serves as an interface variable
 396 between seismology and structural engineering. Several metrics are available in the literature
 397 to be considered as IMs; they can be divided into two broad categories, namely asset-aware
 398 (e.g., spectral accelerations) and asset-agnostic (e.g., peak ground acceleration), either scalar or
 399 vector. In this study, a facility-wide application is presented; hence the selected IM should cover
 400 a spectrum of assets with essentially different geometric and dynamic properties. Using
 401 structure-specific IMs for each considered asset (with potentially increased efficiency and
 402 sufficiency) would lead to the formulation of a rather complicated and even impractical risk
 403 assessment framework for the refinery as an integrated system, at a minimum requiring vector
 404 hazard analysis[85]. Two IMs are proposed for the facility-level application: (1) the average
 405 spectral acceleration over a range of periods, AvgSA, i.e., a moderately asset-aware IM, and (2)
 406 the Peak Ground Acceleration, PGA [37,86] that is adopted as being familiar to most operators.

407 The plant's condition is evaluated at four distinct levels of PGA, namely 0.08g, 0.16g,
 408 0.24g, and 0.36g. The three latter levels correspond to the EN 1998 (Eurocode 8) PGA design
 409 values for Significant Damage (10% probability of exceedance in 50 years) for the three seismic
 410 zones of Greece, while the lowest level is equivalent to the Damage Limitation (50% probability
 411 of exceedance in 50 years) for the lower PGA value of 0.16g, being actually 50% of it.

412 Per the assigned fragilities, each asset has a distinct probability of being in each asset-
 413 specific ds. For example, the results for an almost full ($FR = 0.95$) liquid storage tank TK-5
 414 are illustrated in Figure 6 for the four IM levels considered. For this FR , it is ds2 that has the
 415 highest probability of occurrence in all cases. This is the “most probable damage state” and,
 416 after being homogenized into the five global DSs of Table 2 (see [62]), it is adopted as a simple
 417 metric to help visualize the impact of each IM level on individual assets.

418 Finding the most probable DS is straightforward for process assets, contrary to storage
 419 assets with random FR . In other words, a single fragility curve per damage state is available for
 420 each process asset (e.g., chimney, building, flare, etc.). Contrarily, N alternative fragility curves
 421 per damage state are available for each storage asset, where N equals the number of fill ratios
 422 examined. For the sake of homogeneous visualization, the combined fragility approach [71]
 423 was adopted, assuming equal weights for the different fill ratios due to the lack of better
 424 information that would have allowed a more elaborate treatment. In more detail, for a given IM
 425 level, the probability of a certain DS occurring is obtained from the partial fragilities (each

426 corresponding to a single FR). Then, the mean probability for this DS is computed from all FRs
 427 considered. This process is carried out for all 5 DSs. The most probable DS is the one with the
 428 highest probability. It is noted that tanks under maintenance are by definition expected to be in
 429 DS0, because in general lower *FR* leads to a lower probability of failure (e.g., [30,62,71]).
 430 Finally, note that this visualization approach will assign the same DS to all similar structures
 431 (i.e., those having the same fragility). This is not necessarily realistic unless there is a high
 432 correlation among said structures. One should interpret such visualization results with care,
 433 treating them only as indicative of a “most probable” behavior that may never happen.



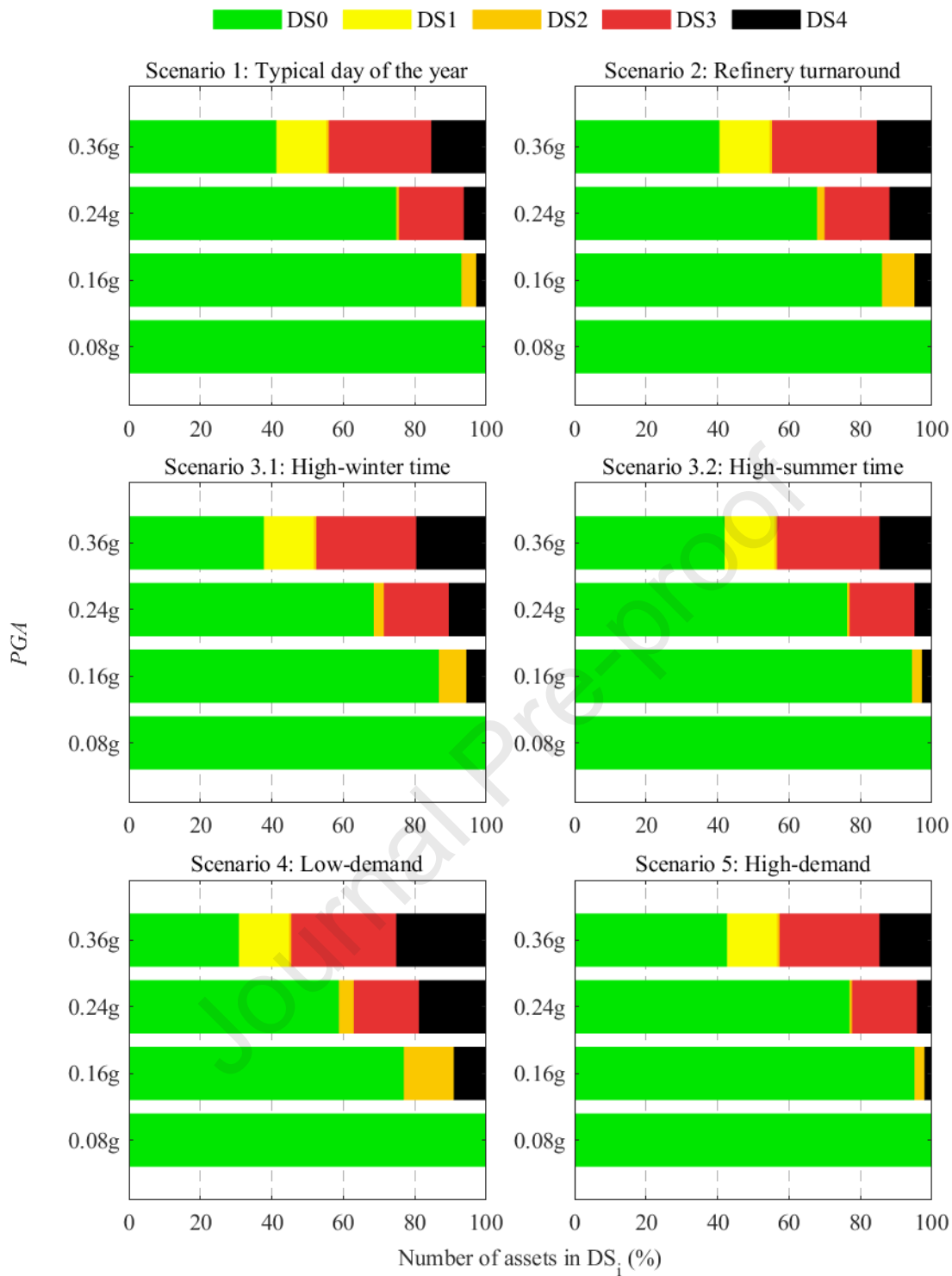
434

435 Figure 6: Liquid storage tank TK-5 with $FR = 0.95$: Probability of exceeding asset-specific
 436 damage states (ds) for predefined levels of seismic intensity.

437 5. Results and discussion

438 5.1 Scenario results

439 An aggregated approach is adopted to evaluate the performance of the refinery: For each
 440 operational scenario and IM level, the most probable DS for each asset is identified and then
 441 all assets of the same DS are binned together. The results are presented in Figure 7 for all
 442 scenarios, where the percentage of assets in each DS is presented on the horizontal axis for the
 443 four considered IM levels, which are shown on the vertical axis. As expected, increasing the
 444 IM level results in an increase of assets being in higher DSs. Overall, the worst-case scenario
 445 is Scenario 4 (low-demand) since the majority of storage assets are more or less full and
 446 consequently more vulnerable to seismically-induced damage. Within the same concept,
 447 Scenario 2 (refinery turnaround), 3.1 (high-winter time), and 4 (low demand) are characterized
 448 by an increased percentage of assets in DS4 (severe level of disruption), which is mainly
 449 attributed to the number of fuel storage assets being full. The number of assets in DS1 (low
 450 level of disruption) and DS2 (moderate level of disruption) is limited; this is indicative of the
 451 narrow window of intensities that can result in such intermediate levels of damage or disruption,
 452 as most assets tend to have non-trivial consequences when damaged [62].

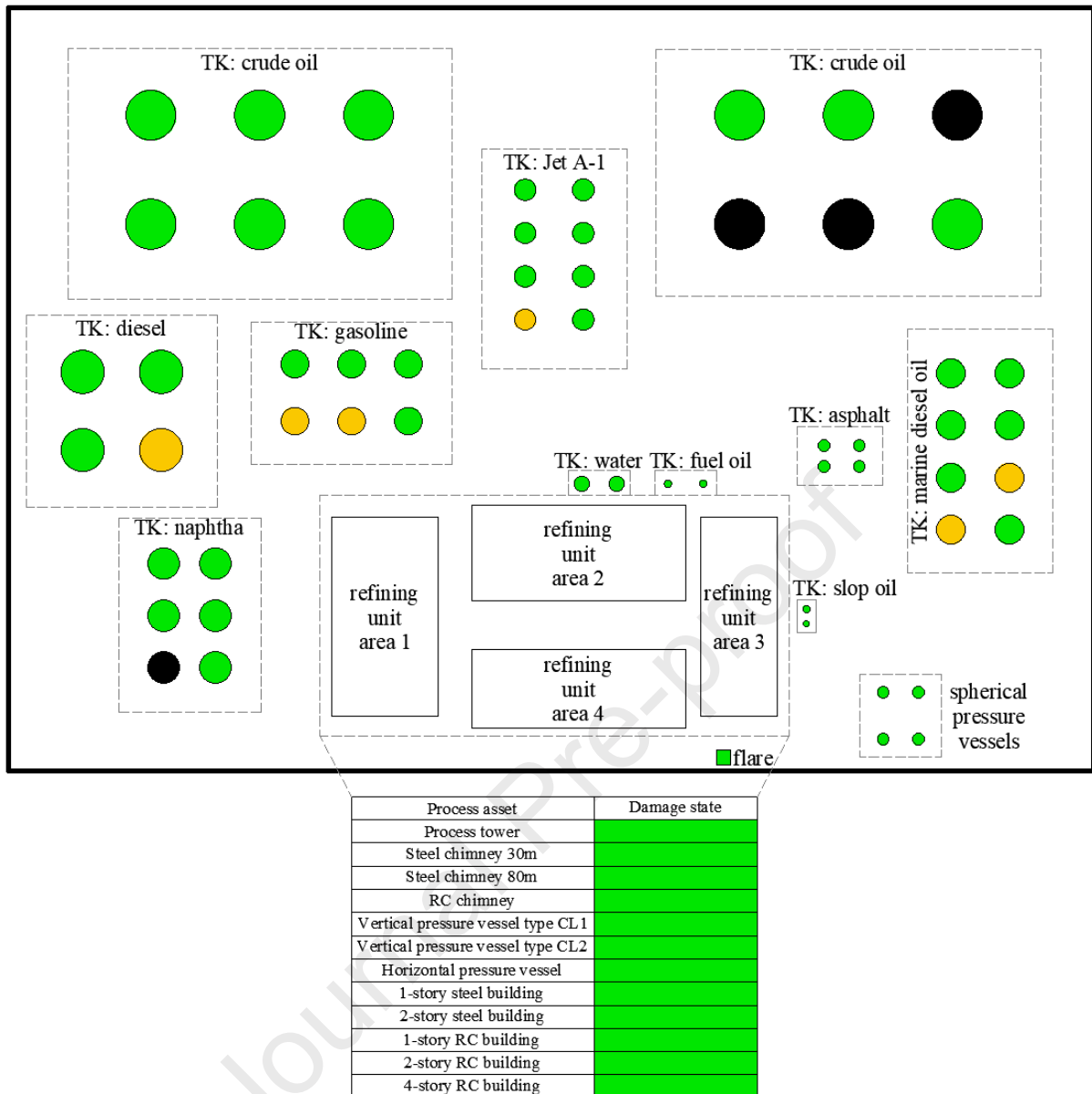


453

454 Figure 7: Percentage of assets in each damage state per scenario for increasing levels of PGA.

455

456 The aggregated results presented in Figure 7 can offer more clarity when viewed in
 457 terms of DS maps. As an all-green map would be rather uninformative, we skip the lowest PGA
 458 level of 0.08g, and turn to the moderate PGA of 0.16g and the “beyond-design” value of 0.36g.
 459 The respective refinery plan views of the most probable DS for Scenario 1 appear in Figure 8
 and Figure 9.



460

461 Figure 8: Scenario 1 (typical day of the year): Most probable DS of assets for $PGA = 0.16g$
 462 [DS0: green, DS1: yellow, DS2: orange, DS3: red, DS4: black].

463

464

465

466

467

468

469

470

471

472

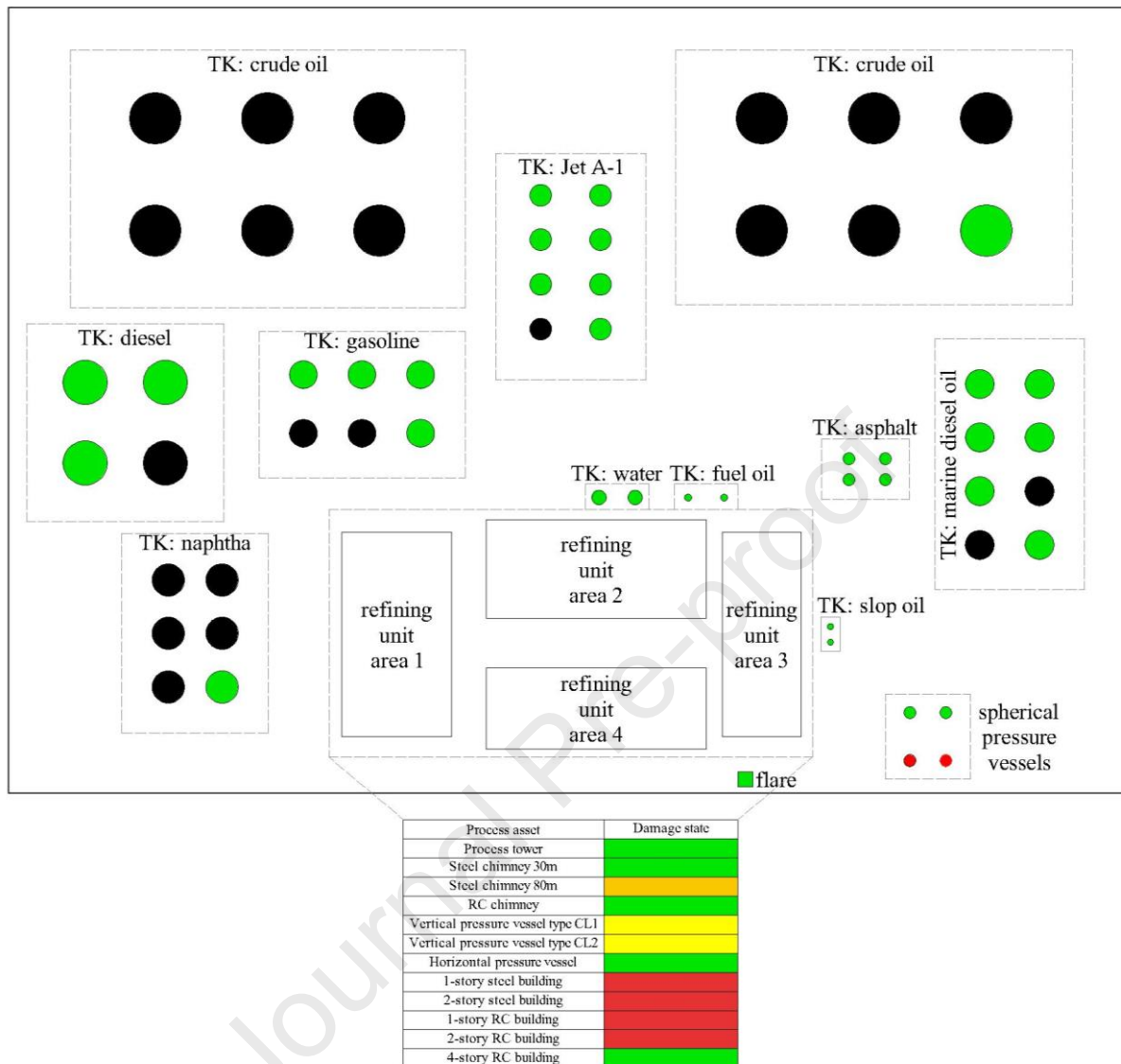
473

474

475

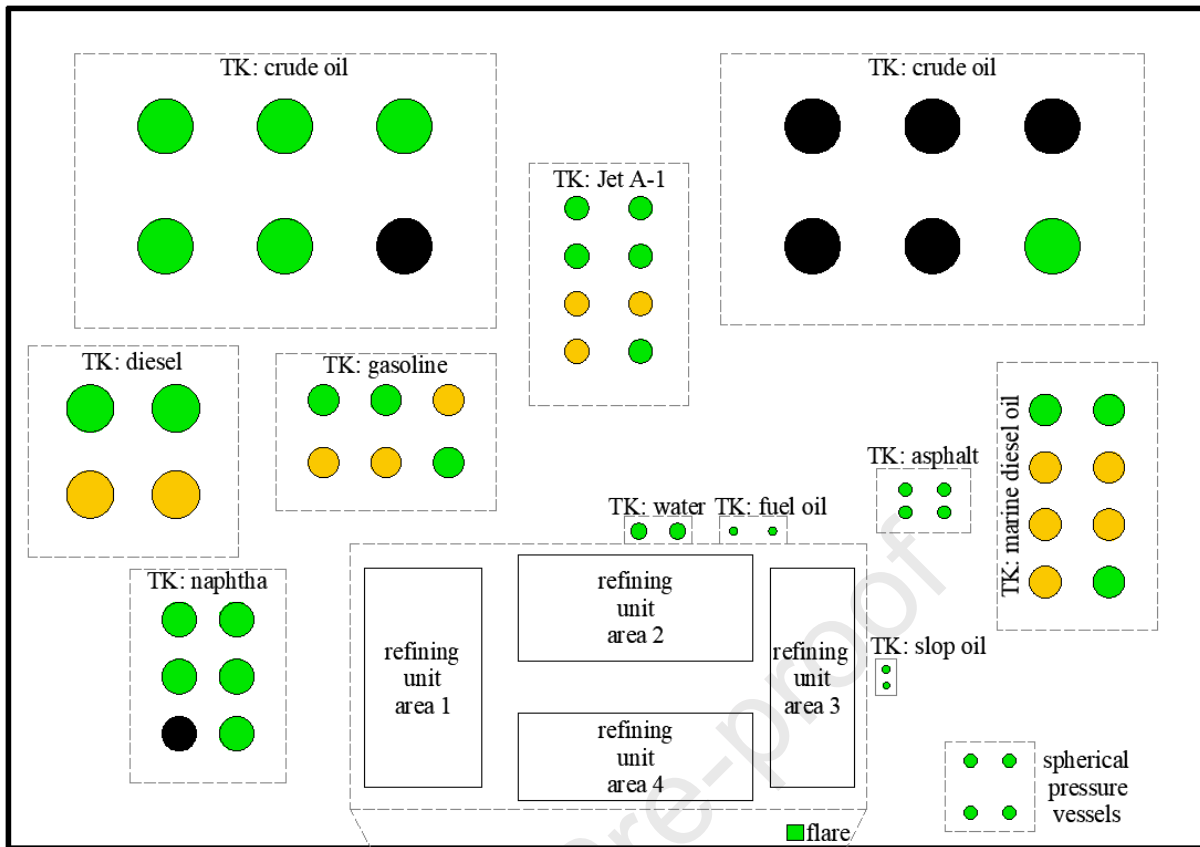
For an earthquake event with $PGA = 0.16g$ (Figure 8) only liquid storage tanks and in particular one naphtha tank and three crude oil tanks are expected to sustain significant damage, while one diesel, two gasoline, and two marine diesel oil tanks are expected to sustain minor damage. Contrarily, no damage is expected within the refining unit areas. Therefore, for this moderate level of seismic intensity within a typical day of refinery operation, one can expect having few tanks that have been damaged with potential loss of containment and triggering of cascading adverse effects, such as a pool fire. If no fire or explosion occurs, any fuel leakage and consequent spills are expected to be contained within the containment berm surrounding each tank [87]. For an earthquake event with an increased intensity, i.e., $PGA = 0.36g$, a large number of assets is expected to suffer significant damage (Figure 9) including several storage and process assets. It is important to identify that (a) two spherical pressure vessels are damaged, which increases the potential for explosion due to the stored high-pressure gas and (b) a lot of equipment is damaged in the equipment-supporting buildings. In the latter case,

476 numerous processes are interrupted and the refining chain is severely broken, while leakage and
 477 fire may break out from failed piping that is attached to the equipment.



478
 479 Figure 9: Scenario 1 (typical day of the year): Most probable DS of assets for $PGA = 0.36g$
 480 [DS0: green, DS1: yellow, DS2: orange, DS3: red, DS4: black].

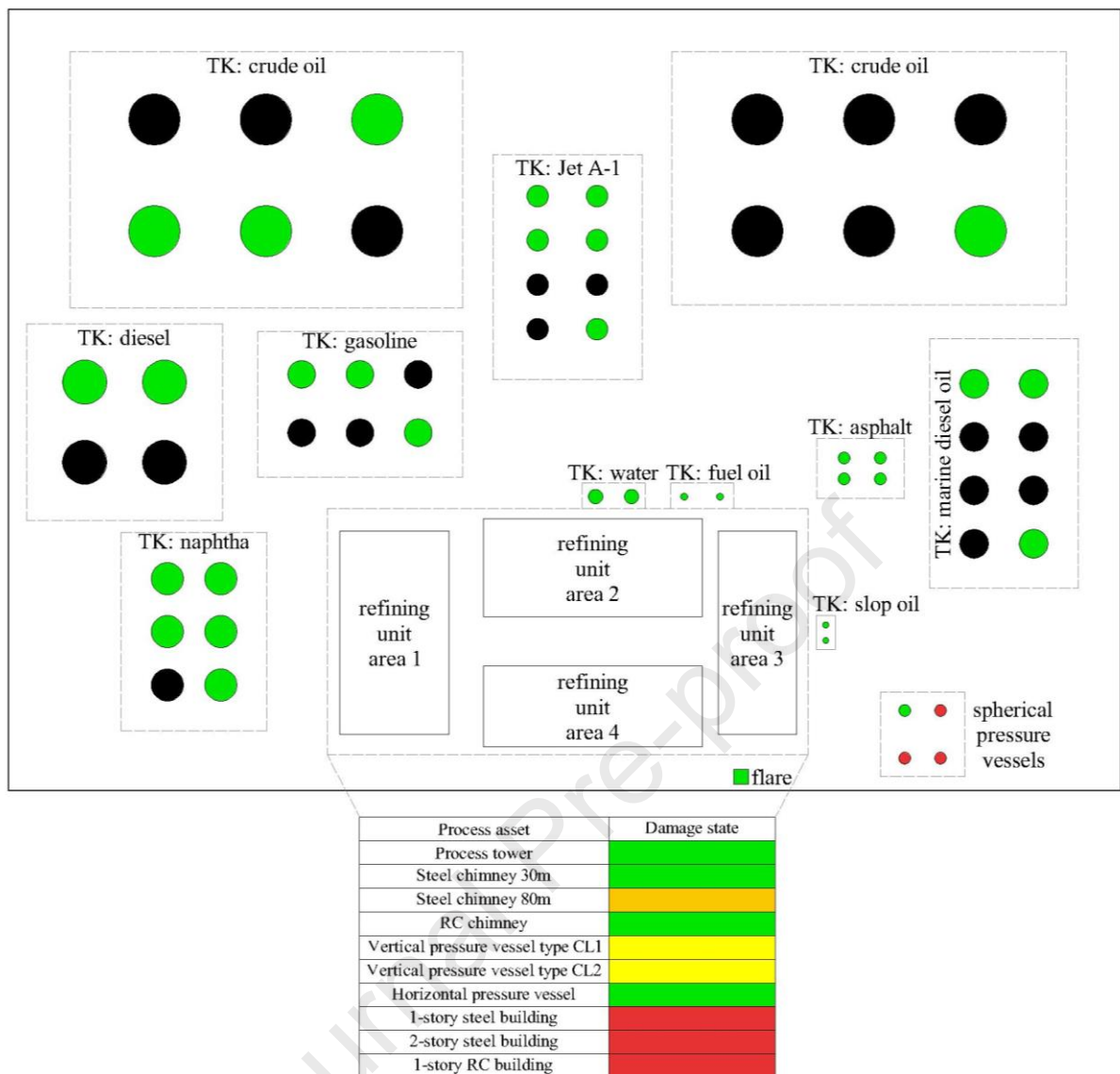
481 The distribution of the failed or non-failed assets within the plant in case of an
 482 earthquake event during the refinery turnaround is shown in Figure 10 considering a seismic
 483 event with a $PGA = 0.16g$ and in Figure 11 for a seismic event with a $PGA = 0.36g$. As
 484 discussed in Section 3.2, during the turnaround period many storage assets are full (Table 5)
 485 and consequently a lot more assets are expected to sustain damage compared to the typical day
 486 scenario (Figure 8). This situation is significantly intensified for increased levels of seismic
 487 intensity, i.e., $PGA = 0.36g$, as shown in Figure 11. The failure of multiple tanks inevitably
 488 increases the potential for catastrophic events, such as explosions, pool fires, and flush fires due
 489 to fuel leakage from tanks. It should be noted that the failure or not of the process assets depends
 490 only on the seismic intensity level, regardless of the operational scenario and therefore the same
 491 conclusions are drawn for Scenarios 1 and 2 per IM level.



Process asset	Damage state
Process tower	DS0
Steel chimney 30m	DS0
Steel chimney 80m	DS0
RC chimney	DS0
Vertical pressure vessel type CL1	DS0
Vertical pressure vessel type CL2	DS0
Horizontal pressure vessel	DS0
1-story steel building	DS0
2-story steel building	DS0
1-story RC building	DS0
2-story RC building	DS0
4-story RC building	DS0

492

493 Figure 10: Scenario 2 (refinery turnaround): Most probable DS of assets for $PGA = 0.16g$
 494 [DS0: green, DS1: yellow, DS2: orange, DS3: red, DS4: black].



495

496 Figure 11: Scenario 2 (refinery turnaround): Most probable DS of assets for $PGA = 0.36g$
 497 [DS0: green, DS1: yellow, DS2: orange, DS3: red, DS4: black].

498 5.2 Combination of scenarios and typical approaches

499

500

501

502

503

504

505

506

507

508

509

510

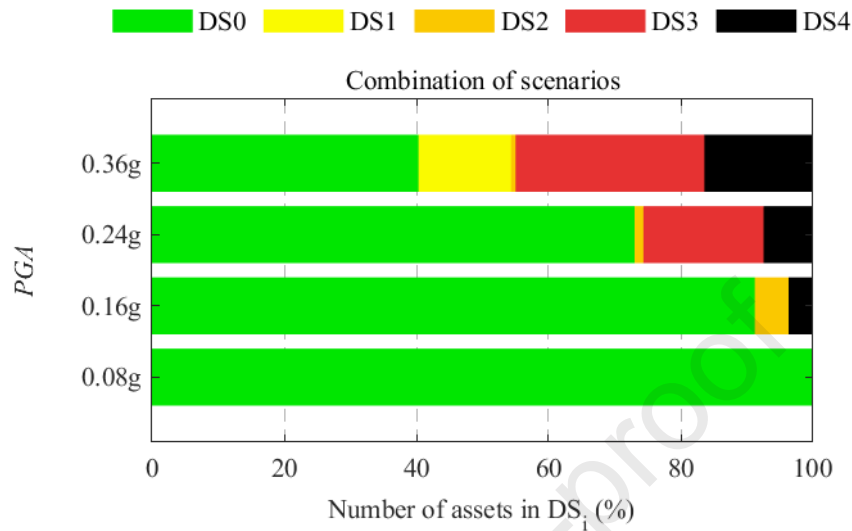
511

512

513

Given the nonlinear nature of the consequences of asset damage, we contend that the superior approach is the direct consideration of individual operational scenarios. For maximum accuracy, the combination of the respective consequences should only be performed downstream, per refinery realization, and on an event-by-event basis, e.g., within the context of event-based probabilistic seismic hazard analysis [88]. Still, one has to recognize that this cannot be the norm in resource-constrained risk assessment studies. There is still some value to having an “averaged” combined scenario using the annualized weights (see Table 10) to provide (approximate) “averaged” estimates in a time-less and scenario-less manner about the expected number of assets in each damage state. Such summarized results can still help stakeholders plan emergency response and prioritize rehabilitation actions. The respective combined estimates are illustrated in Figure 12. In comparison to Figure 7, Scenarios 1 and 3 now dominate the results because their time span is the longest within the refinery schedule. Still, one should not focus on just the grand picture presented by such summarized graphs. It is not only the number of damaged assets but also their location and type; despite the homogenization of the DSs employed, some assets may still lead to significant downtime and monetary losses when

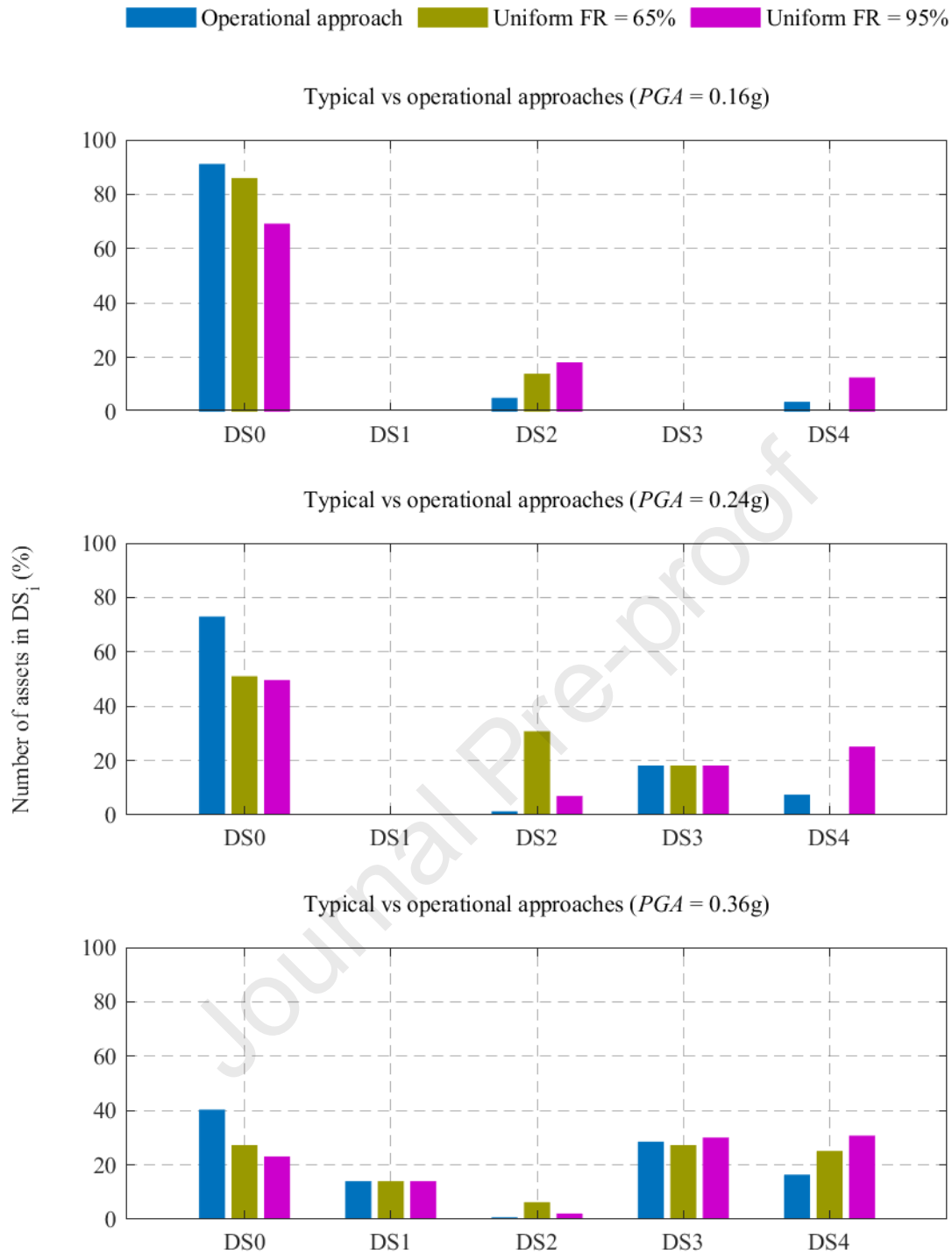
514 considering cascading events at the facility level (e.g., [89,90]). Finally, note that one can also
 515 generate a map of the most probable DS for the combined scenario, similar to the ones of Figure
 516 8 to Figure 11. As long as it is understood that this would be a composite of multiple actual
 517 realizations, with little chance of it ever actually occurring, it can still serve as a useful
 518 “heatmap” for weak spots. For reasons of brevity, it is not shown herein.



519
 520 Figure 12: Weighted average percentage of assets in each damage state for all scenarios for
 521 increasing levels of PGA.

522 After examining the effect of the operational status of the refinery on the seismic
 523 performance estimates, it is worth comparing the results with the typical approach of a uniform
 524 fill ratio (e.g., [55,58]). To do so, two options are considered regarding the fill ratio of storage
 525 assets, namely a uniform FR at 65% and at 95%, i.e., storage assets are considered all to be
 526 either above half-full or almost full. High FR values are often adopted for reasons of
 527 conservativeness, with 95% being a usual choice by virtue of reflecting the worst-case scenario.

528 The comparison between the combined-scenario variable-FR Operational Approach and
 529 the typical uniform-FR approaches appears in Figure 13 for $PGA = 0.16g, 0.24g,$ and $0.36g$.
 530 As expected, regardless of the PGA level, considering a (high) uniform FR leads to an
 531 overestimation of damage. In case of $FR = 0.95$, few undamaged assets (DS0) are observed,
 532 while there is an overestimation of severe failures (DS3 & DS4). For $FR = 0.65$, an increased
 533 number of assets in DS2 is observed, while failures (DS4) are underestimated for lower PGA
 534 values. In general, there is no “perfect” uniform FR value one can employ. Moreover, this
 535 comparison illustrates that, for frequent events of low seismic intensity, considering a uniform
 536 FR for storage assets can lead to more conservative damage estimates that may affect the
 537 insurance cost of the process plant.



538

539 Figure 13: Number of assets (%) in each DS for increasing levels of PGA: Comparison of the
 540 combined-scenario operational approach to typical approaches with uniform fill ratio of storage
 541 assets.

542

543 6. Conclusions

544 The reliable estimation of seismic risk and resilience of oil refineries is essential to
 545 ensure their operability in the aftermath of an earthquake event, to set insurance premiums, and
 546 to develop, upgrade, and update emergency response plans. To do so, an open-data testbed
 547 developed by the authors [62] has been used to consider the actual operational status of the
 548 plant. Alternative scenarios are considered accounting for the effect of seasonality, periods of

549 low and high demand, as well as periods of maintenance. These may not affect the behavior of
550 assets associated with the refining process, but invariably determine the (distribution of) fill
551 ratio for fuel-storage assets, which are typically the ones that carry the more severe cascading
552 consequences.

553 Although cascading damages and domino effects are not addressed per se, their
554 initiating events are studied in detail. Overall, the effect of the plant's operational status is
555 substantial, as it largely determines the number, type, and location of assets that are expected
556 to fail due to the ground shaking. The distribution of asset failure within the refinery plan offers
557 an insight into the locations where cascading failures may be triggered and assists stakeholders
558 in developing customized plans and businesslike procedures for emergency response actions
559 and preventive measures. Moreover, the comparison of operational status results to the typical
560 assessment approaches, where all storage assets are considered to be full or have a conservative
561 uniform fill ratio, demonstrates that the latter approach leads to an excessive estimate of damage
562 and it certainly cannot reflect the refinery's actual vulnerability. As a final remark, the results
563 may not be directly applicable to other refining facilities, but the concept is. The aim and core
564 novelty of the study is the introduction of the refinery operational status concept, which cannot
565 be discounted when performing a comprehensive seismic risk assessment study for such critical
566 facilities. Furthermore, open analysis data published by the authors for typical refinery
567 structural systems [62,63] enable the combination thereof to study cascading effects and form
568 alternative case studies in the future.

569

570 **CRedit authorship contribution statement**

571 **V.E. Melissianos:** Conceptualization, Methodology, Data curation, Supervision, Validation,
572 Formal analysis, Visualization, Writing – original draft, Writing – review & editing. **N.D.**
573 **Karaferis:** Conceptualization, Validation, Formal analysis, Data curation, Methodology,
574 Visualization, Writing – original draft, Writing – review & editing. **K. Bakalis:**
575 Conceptualization, Formal analysis, Data curation, Validation, Writing – review & editing.
576 **A.K. Kazantzi:** Conceptualization, Validation, Formal analysis, Data curation, Supervision,
577 Writing – review & editing. **D. Vamvatsikos:** Conceptualization, Validation, Methodology,
578 Project administration, Supervision, Writing – review & editing, Funding acquisition.

579

580 **Declarations of Conflicting Interests**

581 The authors declare that they have no known competing financial interests or personal
582 relationships that could have appeared to influence the work reported in this paper.

583

584 **Acknowledgments**

585 The authors would like to thank all practitioners and refinery experts who offered information
586 on refinery operation procedures.

587

588 **Funding**

589 This research has been co-financed by the European Union through the HORIZON 2020
590 research and innovation programme “METIS–Seismic Risk Assessment for Nuclear Safety”
591 under Grant Agreement No. 945121 and the HORIZON innovation action “PLOT0–

592 Deployment and Assessment of Predictive modelling, environmentally sustainable and
593 emerging digital technologies and tools for improving the resilience of IWW against Climate
594 change and other extremes” under Grant Agreement No. 101069941.

595

596 **Data availability**

597 Source data is available at <https://doi.org/10.5281/zenodo.11419659>. Data generated in this
598 study will be made available upon reasonable request.

599

600 **ORCID IDs**

601 Vasileios E. Melissianos <https://orcid.org/0000-0002-1589-0697>

602 Nikolaos D. Karaferis <https://orcid.org/0000-0001-9783-7672>

603 Konstantinos Bakalis <https://orcid.org/0000-0002-0826-1059>

604 Athanasia K. Kazantzi <https://orcid.org/0000-0002-5233-6740>

605 Dimitrios Vamvatsikos <https://orcid.org/0000-0002-4016-5040>

606

607 **References**

- 608 [1] A.M. Cruz, L.J. Steinberg, Industry preparedness for earthquakes and earthquake-
609 triggered hazmat accidents in the 1999 Kocaeli earthquake, *Earthquake Spectra* 21
610 (2005) 285–303. <https://doi.org/10.1193/1.1889442>
- 611 [2] European Union, DIRECTIVE 2012/18/EU OF THE EUROPEAN PARLIAMENT
612 AND OF THE COUNCIL of 4 July 2012 on the control of major-accident hazards
613 involving dangerous substances, amending and subsequently repealing Council
614 Directive 96/82/EC, European Parliament, Brussels, 2012. [https://eur-](https://eur-lex.europa.eu/legal-content/EN/TXT/PDF/?uri=CELEX:32012L0018)
615 [lex.europa.eu/legal-content/EN/TXT/PDF/?uri=CELEX:32012L0018](https://eur-lex.europa.eu/legal-content/EN/TXT/PDF/?uri=CELEX:32012L0018) (accessed June
616 21, 2024)
- 617 [3] D. Mitchell, R. Tinawi, Structural damage due to the April 22, 1991, Costa Rican
618 earthquake, 1992. www.nrcresearchpress.com
- 619 [4] H. Sezen, A.S. Whittaker, Seismic performance of industrial facilities affected by the
620 1999 Turkey earthquake, *Journal of Performance of Constructed Facilities* 20 (2006)
621 28–36. [https://doi.org/10.1061/\(ASCE\)0887-3828\(2006\)20:1\(28\)](https://doi.org/10.1061/(ASCE)0887-3828(2006)20:1(28))
- 622 [5] K. Hatayama, Damage to oil storage tanks from the 2011 Mw 9.0 Tohoku-Oki tsunami,
623 *Earthquake Spectra* 31 (2015) 1103–1124. <https://doi.org/10.1193/050713EQS120M>
- 624 [6] C. Naito, D. Cox, Q.-S. “Kent” Yu, H. Brooker, Fuel storage container performance
625 during the 2011 Tohoku, Japan, Tsunami, *Journal of Performance of Constructed*
626 *Facilities* 27 (2013) 373–380. [https://doi.org/10.1061/\(asce\)cf.1943-5509.0000339](https://doi.org/10.1061/(asce)cf.1943-5509.0000339)
- 627 [7] E. Krausmann, A.M. Cruz, Natech risk management in Japan after Fukushima – What
628 have we learned?, *Loss Prevention Bulletin* (2021) 10–14.
629 <https://www.icheme.org/media/15301/krausmannnew.pdf> (accessed November 14,
630 2022)
- 631 [8] S. Eshghi, M.S. Razzaghi, Performance of industrial facilities in the 2003 Bam, Iran,
632 earthquake, *Earthquake Spectra* 21 (2005) 395–410. <https://doi.org/10.1193/1.2098810>

- 633 [9] S. Miladi, M. S. Razzaghi, Failure analysis of an un-anchored steel oil tank damaged
634 during the Silakhor earthquake of 2006 in Iran, *Eng Fail Anal* 96 (2019) 31–43.
635 <https://doi.org/10.1016/j.engfailanal.2018.09.031>
- 636 [10] E. Krausmann, A. Maria, B. Affeltranger, The impact of the 12 May 2008 Wenchuan
637 earthquake on industrial facilities, *J Loss Prev Process Ind* 23 (2010) 242–248.
638 <https://doi.org/10.1016/j.jlp.2009.10.004>
- 639 [11] R. Tremblay, D. Mitchell, R. Tinawi, Damage to industrial structures due to the 27
640 February 2010 Chile earthquake, *Canadian Journal of Civil Engineering* 40 (2013)
641 735–749. <https://doi.org/10.1139/cjce-2012-0197>
- 642 [12] L. Liberatore, L. Sorrentino, D. Liberatore, L.D. Decanini, Failure of industrial
643 structures induced by the Emilia (Italy) 2012 earthquakes, *Eng Fail Anal* 34 (2013)
644 629–647. <https://doi.org/10.1016/j.engfailanal.2013.02.009>
- 645 [13] S. Öztürk, E. Altunsu, O. Güneş, A. Sarı, Investigation of industrial structure
646 performances in the Hatay and Gaziantep provinces during the Türkiye earthquakes on
647 February 6, 2023, *Soil Dynamics and Earthquake Engineering* 179 (2024).
648 <https://doi.org/10.1016/j.soildyn.2024.108569>
- 649 [14] A. Labib, M.J. Harris, Learning how to learn from failures: The Fukushima nuclear
650 disaster, *Eng Fail Anal* 47 (2015) 117–128.
651 <https://doi.org/10.1016/j.engfailanal.2014.10.002>
- 652 [15] E. Hollnagel, Y. Fujita, The Fukushima disaster - System failures as the lack of
653 resilience, *Nuclear Engineering and Technology* 45 (2013) 13–20.
654 <https://doi.org/10.5516/NET.03.2011.078>
- 655 [16] United Nations, Sendai Framework for Disaster Risk Reduction 2015 - 2030, Geneva,
656 Switzerland, 2015. www.unisdr.org
- 657 [17] UNISDR, Words into Action Guidelines: National Disaster Risk Assessment
658 (Governance System, Methodologies, and Use of Results), 2017.
659 https://www.unisdr.org/files/globalplatform/591f213cf2fbe52828_wordsintoactionguideline.nationaldi.pdf
- 660
- 661 [18] S.-P.M. Camila, M. Perreur, F. Munoz, A.M. Cruz, Systematic literature review and
662 qualitative meta-analysis of Natech research in the past four decades, *Saf Sci* 116
663 (2019) 58–77. <https://doi.org/10.1016/j.ssci.2019.02.033>
- 664 [19] E. Krausmann, S. Girgin, A. Necci, Natural hazard impacts on industry and critical
665 infrastructure: Natech risk drivers and risk management performance indicators,
666 *International Journal of Disaster Risk Reduction* 40 (2019) 101163.
667 <https://doi.org/10.1016/j.ijdr.2019.101163>
- 668 [20] M. Theocharidou, G. Giannopoulos, Risk assessment methodologies for critical
669 infrastructure protection . Part II : A new approach, Publications of the European
670 Union, Luxembourg, 2015. <https://doi.org/10.2788/621843>
- 671 [21] E. Krausmann, V. Cozzani, E. Salzano, E. Renni, Industrial accidents triggered by
672 natural hazards: An emerging risk issue, *Natural Hazards and Earth System Science* 11
673 (2011) 921–929. <https://doi.org/10.5194/nhess-11-921-2011>

- 674 [22] G. Fabbrocino, I. Iervolino, F. Orlando, E. Salzano, Quantitative risk analysis of oil
675 storage facilities in seismic areas, *J Hazard Mater* 123 (2005) 61–69.
676 <https://doi.org/10.1016/j.jhazmat.2005.04.015>
- 677 [23] C.A. Cornell, H. Krawinkler, Progress and challenges in seismic performance
678 assessment, *PEER Center News* 3 (2000) 1–4.
679 <https://apps.peer.berkeley.edu/news/2000spring/index.html>
- 680 [24] K. Bakalis, D. Vamvatsikos, M. Fragiadakis, Seismic risk assessment of liquid storage
681 tanks via a nonlinear surrogate model, *Earthq Eng Struct Dyn* 46 (2017) 2851–2868.
682 <https://doi.org/10.1002/eqe.2939>
- 683 [25] S. Zuluaga Mayorga, M. Sánchez-Silva, O.J. Ramírez Olivar, F. Muñoz Giraldo,
684 Development of parametric fragility curves for storage tanks: A Natech approach,
685 *Reliab Eng Syst Saf* 189 (2019) 1–10. <https://doi.org/10.1016/j.ress.2019.04.008>
- 686 [26] M. Pourghafari, M. Pourgol-mohammad, R. Alizadeh, M.R. Kaleibar, M. Soleimani,
687 Deterministic hazard assessment for petroleum refinery products storage tanks: Case
688 study of Tabriz refinery, in: *ASME 2017 International Mechanical Engineering*
689 *Congress and Exposition*, ASME, Tampa, FL, USA, 2017: pp. IMECE2017-71139.
690 <https://doi.org/10.1115/IMECE2017-71139>
- 691 [27] J.I. Chang, C.C. Lin, A study of storage tank accidents, *J Loss Prev Process Ind* 19
692 (2006) 51–59. <https://doi.org/10.1016/j.jlp.2005.05.015>
- 693 [28] W. Jing, J. Shen, X. Cheng, W. Yang, Seismic responses of a liquid storage tank
694 considering structure-soil-structure interaction, *Structures* 45 (2022) 2137–2150.
695 <https://doi.org/10.1016/j.istruc.2022.10.003>
- 696 [29] M. Kohrangi, K. Bakalis, G. Triantafyllou, D. Vamvatsikos, P. Bazzurro, Hazard
697 consistent record selection procedures accounting for horizontal and vertical
698 components of the ground motion: Application to liquid storage tanks, *Earthq Eng*
699 *Struct Dyn* 52 (2023) 1232–1251. <https://doi.org/10.1002/eqe.3813>
- 700 [30] K. Bakalis, M. Fragiadakis, D. Vamvatsikos, Surrogate modeling for the seismic
701 performance assessment of liquid storage tanks, *Journal of Structural Engineering* 143
702 (2017) 04016199. [https://doi.org/10.1061/\(ASCE\)ST.1943-541X.0001667](https://doi.org/10.1061/(ASCE)ST.1943-541X.0001667)
- 703 [31] K. Bakalis, S.A. Karamanos, Uplift mechanics of unanchored liquid storage tanks
704 subjected to lateral earthquake loading, *Thin-Walled Structures* 158 (2021) 107145.
705 <https://doi.org/10.1016/j.tws.2020.107145>
- 706 [32] K. Bakalis, M. Kohrangi, D. Vamvatsikos, Seismic intensity measures for above-
707 ground liquid storage tanks, *Earthq Eng Struct Dyn* 47 (2018) 1844–1863.
708 <https://doi.org/10.1002/eqe.3043>
- 709 [33] N.D. Karaferis, A.K. Kazantzi, V.E. Melissianos, K. Bakalis, D. Vamvatsikos, Seismic
710 fragility assessment of high-rise stacks in oil refineries, *Bulletin of Earthquake*
711 *Engineering* 20 (2022) 6877–6900. <https://doi.org/10.1007/s10518-022-01472-2>
- 712 [34] C. Zhou, M. Tian, K. Guo, Seismic partitioned fragility analysis for high-rise RC
713 chimney considering multidimensional ground motion, *Structural Design of Tall and*
714 *Special Buildings* 28 (2019) 1–14. <https://doi.org/10.1002/tal.1568>

- 715 [35] Y. Qiu, C. Zhou, S. A, Correlation between earthquake intensity parameters and
716 damage indices of high-rise RC chimneys, *Soil Dynamics and Earthquake Engineering*
717 137 (2020) 106282. <https://doi.org/10.1016/j.soildyn.2020.106282>
- 718 [36] H. Moharrami, M.A. Amini, Seismic vulnerability assessment of process towers using
719 fragility curves, *The Structural Design of Tall and Special Buildings* 23 (2014) 593–
720 603. <https://doi.org/10.1002/tal.1067>
- 721 [37] A.K. Kazantzi, N.D. Karaferis, V.E. Melissianos, K. Bakalis, D. Vamvatsikos, Seismic
722 fragility assessment of building-type structures in oil refineries, *Bulletin of Earthquake*
723 *Engineering* 20 (2022) 6853–6876. <https://doi.org/10.1007/s10518-022-01476-y>
- 724 [38] C. Butenweg, O.S. Bursi, F. Paolacci, M. Marinković, I. Lanese, C. Nardin, G. Quinci,
725 Seismic performance of an industrial multi-storey frame structure with process
726 equipment subjected to shake table testing, *Eng Struct* 243 (2021) 112681.
727 <https://doi.org/http://dx.doi.org/10.1016/j.engstruct.2021.112681>
- 728 [39] A.K. Kazantzi, N.D. Karaferis, V.E. Melissianos, D. Vamvatsikos, Acceleration-
729 sensitive ancillary elements in industrial facilities: alternative seismic design
730 approaches in the new Eurocode, *Bulletin of Earthquake Engineering* 22 (2024) 109–
731 132. <https://doi.org/10.1007/s10518-023-01656-4>
- 732 [40] C. Butenweg, B. Holtschoppen, Seismic Design of Industrial Facilities in Germany, in:
733 S. Klinkel, C. Butenweg, G. Lin, B. Holtschoppen (Eds.), *Seismic Design of Industrial*
734 *Facilities*, Springer Fachmedien Wiesbaden, Wiesbaden, 2014: pp. 63–74.
735 https://doi.org/10.1007/978-3-658-02810-7_6
- 736 [41] A.M. Alfanda, K. Dai, J. Wang, Review of Seismic Fragility and Loss Quantification of
737 Building-Like Industrial Facilities, *J Press Vessel Technol* 144 (2022).
738 <https://doi.org/10.1115/1.4054844>
- 739 [42] A. Kalantari, D. Abdi, B. Abbasi Feshki, Seismic fragility assessment of equipment and
740 support structure in a unit of a petrochemical plant, *SN Appl Sci* 2 (2020).
741 <https://doi.org/10.1007/s42452-020-3159-4>
- 742 [43] L. Di Sarno, G. Karagiannakis, Seismic performance-based assessment of a RC pipe
743 rack accounting for dynamic interaction, *Structures* 33 (2021) 4604–4615.
744 <https://doi.org/10.1016/j.istruc.2021.07.031>
- 745 [44] L. Di Sarno, G. Karagiannakis, Seismic Assessment of Pipe Racks Accounting for Soil-
746 Structure Interaction, *International Journal of Steel Structures* 20 (2020) 1929–1944.
747 <https://doi.org/10.1007/s13296-020-00393-7>
- 748 [45] L. Di Sarno, G. Karagiannakis, Petrochemical Steel Pipe Rack: Critical Assessment of
749 Existing Design Code Provisions and a Case Study, *International Journal of Steel*
750 *Structures* 20 (2020) 232–246. <https://doi.org/10.1007/s13296-019-00280-w>
- 751 [46] L. Di Sarno, G. Karagiannakis, On the seismic fragility of pipe rack—piping systems
752 considering soil–structure interaction, *Bulletin of Earthquake Engineering* 18 (2020)
753 2723–2757. <https://doi.org/10.1007/s10518-020-00797-0>
- 754 [47] G. Karagiannakis, L. Di Sarno, A. Necci, E. Krausmann, Seismic risk assessment of
755 supporting structures and process piping for accident prevention in chemical facilities,

- 756 International Journal of Disaster Risk Reduction 69 (2022).
757 <https://doi.org/10.1016/j.ijdrr.2021.102748>
- 758 [48] O.S. Bursi, M.S. Reza, G. Abbiati, F. Paolacci, Performance-based earthquake
759 evaluation of a full-scale petrochemical piping system, *J Loss Prev Process Ind* 33
760 (2015) 10–22. <https://doi.org/10.1016/j.jlp.2014.11.004>
- 761 [49] O.S. Bursi, F. Paolacci, M.S. Reza, S. Alessandri, N. Tondini, Seismic assessment of
762 petrochemical piping systems using a performance-based approach, *J Press Vessel*
763 *Technol* 138 (2016) 031801. <https://doi.org/10.1115/1.4032111>
- 764 [50] M. Campedel, V. Cozzani, A. Garcia-Agreda, E. Salzano, Extending the quantitative
765 assessment of industrial risks to earthquake effects, *Risk Analysis* 28 (2008) 1231–
766 1246. <https://doi.org/10.1111/j.1539-6924.2008.01092.x>
- 767 [51] S. Girgin, E. Krausmann, RAPID-N: Rapid natech risk assessment and mapping
768 framework, *J Loss Prev Process Ind* 26 (2013) 949–960.
769 <https://doi.org/10.1016/j.jlp.2013.10.004>
- 770 [52] O.S. Bursi, R. di Filippo, V. La Salandra, M. Pedot, M.S. Reza, Probabilistic seismic
771 analysis of an LNG subplant, *J Loss Prev Process Ind* 53 (2018) 45–60.
772 <https://doi.org/10.1016/j.jlp.2017.10.009>
- 773 [53] S. Alessandri, A.C. Caputo, D. Corritore, R. Giannini, F. Paolacci, H.N. Phan,
774 Probabilistic risk analysis of process plants under seismic loading based on Monte
775 Carlo simulations, *J Loss Prev Process Ind* 53 (2018) 136–148.
776 <https://doi.org/10.1016/j.jlp.2017.12.013>
- 777 [54] A.C. Caputo, F. Paolacci, O.S. Bursi, R. Giannini, Problems and Perspectives in
778 Seismic Quantitative Risk Analysis of Chemical Process Plants, *Journal of Pressure*
779 *Vessel Technology, Transactions of the ASME* 141 (2019).
780 <https://doi.org/10.1115/1.4040804>
- 781 [55] A.C. Caputo, B. Kalemi, F. Paolacci, D. Corritore, Computing resilience of process
782 plants under Na-Tech events: Methodology and application to seismic loading
783 scenarios, *Reliab Eng Syst Saf* 195 (2020) 106685.
784 <https://doi.org/10.1016/j.ress.2019.106685>
- 785 [56] K. Huang, G. Chen, Y. Yang, P. Chen, An innovative quantitative analysis methodology
786 for Natech events triggered by earthquakes in chemical tank farms, *Saf Sci* 128 (2020)
787 104744. <https://doi.org/10.1016/j.ssci.2020.104744>
- 788 [57] D. Corritore, F. Paolacci, S. Caprinuzzi, A Screening Methodology for the
789 Identification of Critical Units in Major-Hazard Facilities Under Seismic Loading,
790 *Front Built Environ* 7 (2021) 780719. <https://doi.org/10.3389/fbuil.2021.780719>
- 791 [58] B. Kalemi, A.C. Caputo, D. Corritore, F. Paolacci, A probabilistic framework for the
792 estimation of resilience of process plants under Na-Tech seismic events, *Bulletin of*
793 *Earthquake Engineering* (2023). <https://doi.org/10.1007/s10518-023-01685-z>
- 794 [59] M. Wang, Z. Sun, J. Sun, Y. Lyu, Y. Wu, Quantitative assessment framework for
795 seismic resilience of petroleum depots, *Structures* 58 (2023) 105400.
796 <https://doi.org/10.1016/j.istruc.2023.105400>

- 797 [60] G.J. O'Reilly, D. Shahnazaryan, P. Dubini, E. Brunesi, A. Rosti, F. Dacarro, A. Gotti,
798 D. Silvestri, S. Mascetti, M. Ducci, M. Ciucci, A. Marino, Risk-aware navigation in
799 industrial plants at risk of NaTech accidents, *International Journal of Disaster Risk*
800 *Reduction* 88 (2023) 103620. <https://doi.org/https://doi.org/10.1016/j.ijdr.2023.103620>
- 801 [61] V.K. Karastathis, D. Diagourtas, D. Vamvatsikos, A. Tselentis, V. Doukas, V.
802 Kapetanidis, K. Boukouras, E. Mouzakiotis, A. Iliakidis, G. Drakatos, N. Karaferis, D.
803 Segura, Early warning system for industrial zone protection. Application in the Eastern
804 Gulf of Corinth, Greece, in: *AGU Annual Meeting 2023*, American Geophysical Union,
805 San Francisco, CA, 2023: pp. S51D-0242.
- 806 [62] V.E. Melissianos, N.D. Karaferis, Bakalis Konstantinos, A.K. Kazantzi, D.
807 Vamvatsikos, Hazard, exposure, fragility, and damage state homogenization of a virtual
808 oil refinery testbed for seismic risk assessment, *Earthquake Spectra* in press (2024).
- 809 [63] V.E. Melissianos, N.D. Karaferis, K. Bakalis, A.K. Kazantzi, D. Vamvatsikos,
810 Exposure and fragility of a virtual oil refinery testbed for seismic risk assessment,
811 *OpenAIRE Project* (2024). <https://doi.org/https://zenodo.org/records/11419659>.
- 812 [64] N. Psyrras, O. Kwon, S. Gerasimidis, A. Sextos, Can a buried gas pipeline experience
813 local buckling during earthquake ground shaking?, *Soil Dynamics and Earthquake*
814 *Engineering* 116 (2019) 511–529. <https://doi.org/10.1016/j.soildyn.2018.10.027>
- 815 [65] S. Farahani, A. Tahershamsi, B. Behnam, Earthquake and post-earthquake vulnerability
816 assessment of urban gas pipelines network, *Natural Hazards* 101 (2020) 327–347.
817 <https://doi.org/10.1007/s11069-020-03874-4>
- 818 [66] T.D. O'Rourke, S.S. Jeon, S. Toprak, M. Cubrinovski, M. Hughes, S. Van Ballegooy,
819 D. Bouziou, Earthquake response of underground pipeline networks in Christchurch,
820 NZ, *Earthquake Spectra* 30 (2014) 183–204. <https://doi.org/10.1193/030413EQS062M>
- 821 [67] R. Basili, L. Danciu, C. Beauval, K. Ssesetyan, S. Vilanova, S. Adamia, P. Arroucau, J.
822 Atanackov, S. Baize, C. Canora, R. Caputo, M. Carafa, M. Cushing, S. Custódio, M.
823 Demircioglu Tumsa, J. Duarte, A. Ganas, J. García-Mayordomo, L. Gómez de la Peña,
824 E. Gràcia, P. Jamšek Rupnik, H. Jomard, V. Kastelic, F. Maesano, R. Martín-Banda, S.
825 Martínez-Lorient, M. Neres, H. Perea, B. Sket-Motnikar, M. Tiberti, N. Tsereteli, V.
826 Tsironi, R. Vallone, K. Vanneste, P. Zupančič, *European Fault-Source Model 2020*
827 *(EFSM20): online data on fault geometry and activity parameters*, Rome, Italy, 2022.
828 <https://doi.org/10.13127/efsm20>
- 829 [68] J. Woessner, D. Laurentiu, D. Giardini, H. Crowley, F. Cotton, G. Grünthal, G.
830 Valensise, R. Arvidsson, R. Basili, M.B. Demircioglu, S. Hiemer, C. Meletti, R.W.
831 Musson, A.N. Rovida, K. Sesetyan, M. Stucchi, The 2013 European Seismic Hazard
832 Model: key components and results, *Bulletin of Earthquake Engineering* 13 (2015)
833 3553–3596. <https://doi.org/10.1007/s10518-015-9795-1>
- 834 [69] A. Boucheikhchoukh, V. Berger, C.L.E. Swartz, A. Deza, A. Nguyen, S. Jaffer,
835 Multiperiod refinery optimization for mitigating the impact of process unit shutdowns,
836 *Comput Chem Eng* 164 (2022). <https://doi.org/10.1016/j.compchemeng.2022.107873>
- 837 [70] H. Moradi, S. Shadrokh, A robust reliability-based scheduling for the maintenance
838 activities during planned shutdown under uncertainty of activity duration, *Comput*
839 *Chem Eng* 130 (2019). <https://doi.org/10.1016/j.compchemeng.2019.106562>

- 840 [71] N.D. Karaferis, V.E. Melissianos, D. Vamvatsikos, Mechanical modeling, seismic
841 fragility, and correlation issues for groups of spherical pressure vessels, *Acta Mech* 235
842 (2023) 1563–1582. <https://doi.org/10.1007/s00707-023-03670-8>
- 843 [72] American Petroleum Institute, API STD 653 Tank inspection, repair, alteration, and
844 reconstruction, Washington, D.C., USA, 2014.
- 845 [73] M. Bevilacqua, F.E. Ciarapica, G. Giacchetta, C. Paciarotti, B. Marchetti, Innovative
846 Maintenance Management Methods in Oil Refineries, in: Springer Series in Reliability
847 Engineering, Springer Science and Business Media Deutschland GmbH, 2016: pp.
848 197–226. https://doi.org/10.1007/978-1-4471-6778-5_7
- 849 [74] A. Hameed, F. Khan, A framework to estimate the risk-based shutdown interval for a
850 processing plant, *J Loss Prev Process Ind* 32 (2014) 18–29.
851 <https://doi.org/10.1016/j.jlp.2014.07.009>
- 852 [75] R.B. Hey, Turnaround Management for the Oil, Gas, and Process Industries, Elsevier,
853 2019. <https://doi.org/10.1016/C2018-0-01138-X>
- 854 [76] J. Inchauspe, J. Li, J. Park, Seasonal patterns of global oil consumption: Implications
855 for long term energy policy, *J Policy Model* 42 (2020) 536–556.
856 <https://doi.org/10.1016/j.jpolmod.2019.12.005>
- 857 [77] R.A. Ratti, J.L. Vespignani, OPEC and non-OPEC oil production and the global
858 economy, *Energy Econ* 50 (2015) 364–378.
859 <https://doi.org/10.1016/j.eneco.2014.12.001>
- 860 [78] B.R. Auer, Daily seasonality in crude oil returns and volatilities, *Energy Econ* 43
861 (2014) 82–88. <https://doi.org/10.1016/j.eneco.2014.02.005>
- 862 [79] S.A. Raza, A.W. Siddiqui, Exploring temporal demand patterns of refined petroleum
863 products: Implications of the COVID-19 pandemic as a black swan event, *Extractive
864 Industries and Society* 17 (2024). <https://doi.org/10.1016/j.exis.2023.101388>
- 865 [80] Q. Wang, F. Zhang, R. Li, L. Li, Forecasting China’s energy demand post-COVID-19
866 pandemic: Insights from energy type differences and regional differences, *Energy
867 Strategy Reviews* 42 (2022). <https://doi.org/10.1016/j.esr.2022.100881>
- 868 [81] S.S. Priya, E. Cuce, K. Sudhakar, A perspective of COVID 19 impact on global
869 economy, energy and environment, *International Journal of Sustainable Engineering* 14
870 (2021) 1290–1305. <https://doi.org/10.1080/19397038.2021.1964634>
- 871 [82] J.J. Bommer, Deterministic vs. probabilistic seismic hazard assessment: An
872 exaggerated and obstructive dichotomy, *Journal of Earthquake Engineering* 6 (2002)
873 43–73. <https://doi.org/10.1080/13632460209350432>
- 874 [83] R.P. Kennedy, M.K. Ravindra, Seismic fragilities for nuclear power plant risk studies,
875 *Nuclear Engineering and Design* 79 (1984) 47–68. [https://doi.org/10.1016/0029-
876 5493\(84\)90188-2](https://doi.org/10.1016/0029-5493(84)90188-2)
- 877 [84] K. Bakalis, D. Vamvatsikos, Seismic fragility functions via nonlinear response history
878 analysis, *Journal of Structural Engineering* 144 (2018) 04018181.
879 [https://doi.org/10.1061/\(ASCE\)ST.1943-541X.0002141](https://doi.org/10.1061/(ASCE)ST.1943-541X.0002141)

- 880 [85] P. Bazzurro, C.A. Cornell, Vector-valued probabilistic seismic hazard analysis,
881 Seismological Research Letters 72 (2001) 273. <https://doi.org/10.1785/gssrl.72.2.207>.
- 882 [86] A.K. Kazantzi, D. Vamvatsikos, Intensity measure selection for vulnerability studies of
883 building classes, Earthq Eng Struct Dyn 44 (2015) 2677–2694.
884 <https://doi.org/10.1002/eqe.2603>
- 885 [87] American Petroleum Insititute, API STD 650: Welded Tanks for Oil Storage,
886 Washington, DC, 2020.
- 887 [88] M. Pagani, D. Monelli, G. Weatherill, L. Danciu, H. Crowley, V. Silva, P. Henshaw, L.
888 Butler, M. Nastasi, L. Panzeri, M. Simionato, D. Vigano, Openquake engine: An open
889 hazard (and risk) software for the global earthquake model, Seismological Research
890 Letters 85 (2014) 692–702. <https://doi.org/10.1785/0220130087>
- 891 [89] E. Durukal, M. Erdik, Physical and economic losses sustained by the industry in the
892 1999 Kocaeli, Turkey earthquake, in: Natural Hazards, 2008: pp. 153–178.
893 <https://doi.org/10.1007/s11069-008-9218-6>
- 894 [90] K. Bakalis, D. Vamvatsikos, N.D. Grant, A. Mistry, Downtime assessment of base-
895 isolated liquid storage tanks, in: SECED 2019, Society for Earthquake and Civil
896 Engineering Dynamics, Greenwich, London, 2019.

897

1 **Operational Status Effect on the Seismic Risk Assessment of Oil Refineries**

2

3 **Vasileios E. Melissianos¹, Nikolaos D. Karaferis¹, Konstantinos Bakalis¹, Athanasia K.**
4 **Kazantzi², Dimitrios Vamvatsikos¹**

5

6 **Declarations of Conflicting Interests**

7 The authors declare that they have no known competing financial interests or personal
8 relationships that could have appeared to influence the work reported in this paper.

9

Journal Pre-proof